Cell

Kr-h1 maintains distinct caste-specific neurotranscriptomes in response to socially regulated hormones

Graphical abstract

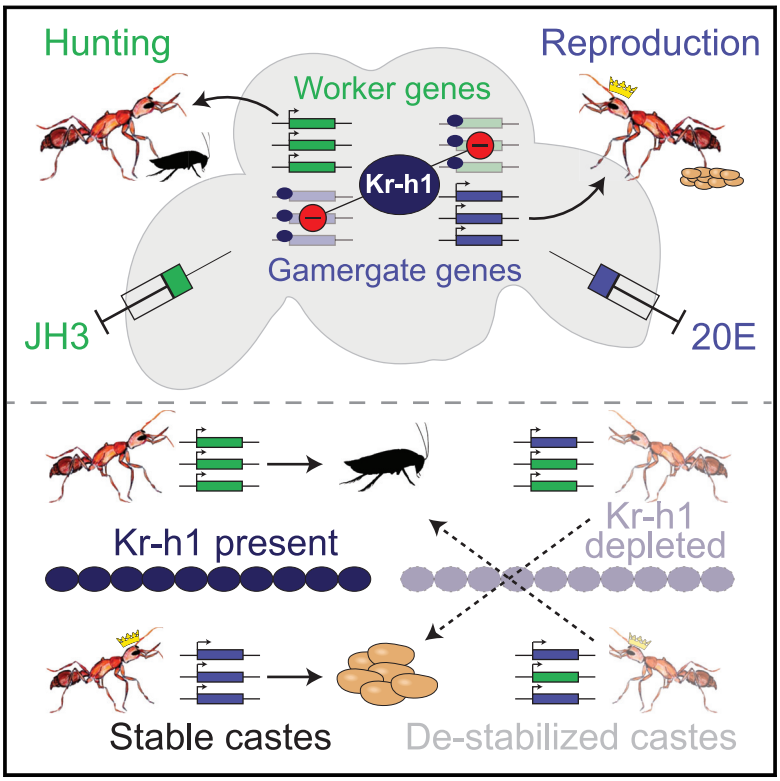

Highlights

- JH3 and 20E drive caste-specific transcription and behavior in *Harpegnathos* ants
- Both JH3 and 20E induce expression of *Kr-h1* in *Harpegnathos* neurons *in vitro*
- Kr-h1 binds to and represses different genes in the brains of different castes
- Knockdown of Kr-h1 destabilizes caste identity and results in inappropriate behavior

Authors

Janko Gospocic, Karl M. Glastad, Lihong Sheng, Emily J. Shields, Shelley L. Berger, Roberto Bonasio

Correspondence

bergers@pennmedicine.upenn.edu (S.L.B.), roberto@bonasiolab.org (R.B.)

In brief

A single transcription factor, Kr-h1, is able to regulate caste identity in *Harpegnathos saltator* by acting as a core transcriptional regulator in response to caste-specific hormone signaling.

Gospocic et al., 2021, Cell *184*, 1–17
November 11, 2021
https://doi.org/10.1016/j.cell.2021.10.006

Cell

CellPress

Article

Kr-h1 maintains distinct caste-specific neurotranscriptomes in response to socially regulated hormones

Janko Gospocic,[1,2,5] Karl M. Glastad,[1,5] Lihong Sheng,[1] Emily J. Shields,[1,2] Shelley L. Berger,[1,3,4,*] and Roberto Bonasio[1,6,*]

[1]Epigenetics Institute and Department of Cell and Developmental Biology, University of Pennsylvania Perelman School of Medicine, Philadelphia, PA 19104, USA

[2]Department of Urology and Institute of Neuropathology, Medical Center-University of Freiburg, Faculty of Medicine, University of Freiburg, Freiburg, Germany

[3]Department of Genetics, University of Pennsylvania Perelman School of Medicine, Philadelphia, PA 19104, USA

[4]Department of Biology, University of Pennsylvania School of Arts and Sciences, Philadelphia, PA 19104, USA

[5]These authors contributed equally

[6]Lead contact

*Correspondence: bergers@pennmedicine.upenn.edu (S.L.B.), roberto@bonasiolab.org (R.B.)

https://doi.org/10.1016/j.cell.2021.10.006

SUMMARY

Behavioral plasticity is key to animal survival. *Harpegnathos saltator* ants can switch between worker and queen-like status (gamergate) depending on the outcome of social conflicts, providing an opportunity to study how distinct behavioral states are achieved in adult brains. Using social and molecular manipulations in live ants and ant neuronal cultures, we show that ecdysone and juvenile hormone drive molecular and functional differences in the brains of workers and gamergates and direct the transcriptional repressor Kr-h1 to different target genes. Depletion of Kr-h1 in the brain caused de-repression of "socially inappropriate" genes: gamergate genes were upregulated in workers, whereas worker genes were upregulated in gamergates. At the phenotypic level, loss of Kr-h1 resulted in the emergence of worker-specific behaviors in gamergates and gamergate-specific traits in workers. We conclude that Kr-h1 is a transcription factor that maintains distinct brain states established in response to socially regulated hormones.

INTRODUCTION

Societies are organized into hierarchies, often through social conflict. Social defeat profoundly impacts animals, with the potential to induce abnormal behavior and disease (Berton et al., 2006; Franklin et al., 2017; Hammels et al., 2015; Mouri et al., 2018; Takahashi et al., 2017). In both mammals and *Drosophila melanogaster*, steroid signaling pathways regulate behavioral responses to social cues (Hashikawa et al., 2017; Ishimoto et al., 2009, 2013; Wei et al., 2004; Yang and Shah, 2014), but the transcriptional mechanisms by which steroids regulate internal brain states remain unclear.

The ant *Harpegnathos saltator* is an excellent model system to study how molecular memories of social experiences establish long-lasting behavioral traits. Unlike most ant species, *Harpegnathos* individuals can change caste through adulthood (Peeters and Hölldobler, 1995). When the queen dies or is removed from a colony, workers enter a dueling tournament until a few become reproductive individuals, called gamergates (Peeters et al., 2000; Sasaki et al., 2016). Gamergates abandon worker tasks such as foraging, lay eggs, and exhibit dominant behaviors toward workers. This behavioral transition is accompanied by a 5-fold lifespan extension, a reconfiguration of gene expression and cellular composition of the brain, and neurohormonal changes (Ghaninia et al., 2017; Gospocic et al., 2017; Penick et al., 2014; Sheng et al., 2020). For example, mature gamergates and foraging workers have different levels of the terpenoid hormone juvenile hormone III (JH3) and the ecdysteroid hormone 20-hydroxyecdysone (20E) (Penick et al., 2011).

JH3 and 20E bind to intracellular receptors—Met and EcR, respectively—that regulate transcription after translocating to the nucleus (Figure S1A). These hormones play important roles in insect metamorphosis (Jindra et al., 2013; Truman, 2019; Yamanaka et al., 2013), but their functions in adult brain and behavioral plasticity are less well characterized. Differences in juvenile hormones and ecdysteroids across castes have been observed in several social insects (Bloch et al., 2000; Brent et al., 2006; Brian, 1974; Rachinsky et al., 1990; Robinson et al., 1991; Wheeler and Nijhout, 1981), and increased levels of JH3 correlate with the age-associated transition to foraging in honeybees and ants (Dolezal et al., 2012; Elekonich et al., 2001; Huang et al., 1991). However, a direct role for JH3 and 20E in regulating

caste-specific behaviors via transcriptional changes has not been demonstrated. One conserved effector of juvenile hormone is the zinc-finger transcription factor Krüppel homolog-1 (Kr-h1) (Lozano and Belles, 2011; Minakuchi et al., 2008, 2009; Ojani et al., 2018). Intriguingly, expression levels of Kr-h1 have been correlated with caste and behavioral differences in social insects (Fussnecker and Grozinger, 2008; Grozinger and Robinson, 2007; Jedlička et al., 2016; Shpigler et al., 2010), but little is known about its function and gene targets in the brain.

We developed and utilized primary ant neuronal cultures to investigate the transcriptional responses of post-mitotic neurons to JH3 or 20E. We combined these *in vitro* studies with social manipulation and functional genomics to reveal a central role of Kr-h1 in mediating the response to JH3 and 20E and enforcing transcriptional boundaries between caste-specific brain states.

RESULTS

JH3 and 20E drive caste-specific gene expression and behavior

We previously compared transcriptomes from whole brains without optic lobes of "generic" *Harpegnathos* workers and gamergates (Gospocic et al., 2017). To increase our power to identify gene expression changes, we analyzed central brains after removing gnathal ganglia and antennal lobes from mature (4 months old) foraging workers and actively reproducing gamergates. In addition to capturing previously identified caste-biased genes (Figure S1B), including *corazonin* in workers and *vitellogenin* in gamergates (Figure 1A, magenta dots), these stricter behavioral definitions and increased anatomical focus resulted in the identification of 2,294 new caste-biased genes, for a total of 2,540 genes differentially expressed between the brains of workers and gamergates (Figure 1A, dark gray dots; Table S1). These genes were enriched for Gene Ontology (GO) terms related to metabolism, development, and neuronal function (Figure S1C; Table S2).

Because of previous studies reporting correlations between juvenile hormone and ecdysteroid titers with caste identity in bees and ants, we searched the *Harpegnathos* RNA sequencing (RNA-seq) data for transcriptional signatures of the two hormones. Among the most upregulated genes in worker brains were three associated with juvenile hormone signaling and function (*Kr-h1*, *hymenoptaecin*, and *to*) (Guo et al., 2020; Lago et al., 2016; Minakuchi et al., 2008) (Figure 1A, green dots), whereas ecdysone-induced protein (EIP) genes (*Eip71CD*, *Eip78C*, and *Eip78Cl*) and the ecdysone-responsive *E23* gene were upregulated in gamergates (Figure 1A, blue dots). This is consistent with the observation that juvenile hormone and ecdysteroid titers are increased in workers and gamergates, respectively (Penick et al., 2011).

Because *Harpegnathos* castes are plastic, we reasoned that administration of JH3 or 20E might be sufficient to initiate a switch in caste-specific transcriptional profiles and behaviors. Injection of JH3 or 20E into the brains of immature (10 days old) workers (Figure 1B) resulted in the differential expression of 885 genes (Figure 1C; Table S1). Known ecdysone-responsive genes (*Eip74EF*, *Eip75B*, *E23*, *Hr3*, and *Hr4*) were induced by 20E (Figure 1C, blue dots), whereas genes associated with juvenile hormone function (e.g., *groucho* [*gro*] and *hairy* [*h*]) (Saha et al., 2016) were upregulated in response to JH3 (Figure 1C, green dots). Two insulin-like peptides (*Ilp1* and *Ilp2*) and an insulin receptor gene (*InR*) were also differentially regulated by JH3 and 20E. The insulin pathway is involved in caste determination (Ament et al., 2008; Jedlička et al., 2016; Wang et al., 2013; Wheeler et al., 2006), and a switch between *Ilp1* and *Ilp2* is key to the transition between foraging and reproduction in the clonal raider ant (Chandra et al., 2018). Consistent with this, *Ilp1* was naturally upregulated in *Harpegnathos* workers and artificially by JH3 injections, whereas *Ilp2* and *InR* were upregulated in gamergates and by 20E injections (Figures 1A and 1C, purple dots).

We hypothesized that JH3 and 20E might promote caste-specific gene expression programs in the brain. We compared the brain transcriptomes from mature workers and gamergates (Figure 1A) with those obtained in response to JH3 and 20E (Figure 1C). A principal component analysis (PCA) revealed that the largest amount of variance separated untreated mature individuals from immature injected workers (Figure 1D, x axis). Strikingly, the second component captured the similarities between the mature castes and the hormone-induced states, with a clear correspondence of worker brains and JH3 on one hand, and gamergate brains and 20E on the other (Figure 1D, y axis). Consistent with this observation, caste-biased genes overlapped extensively with genes responsive to JH3 or 20E stimulation (Figures 1E and S1D). Compared to the DMSO control, JH3 injections promoted a worker-like transcriptional state (Figure 1F), whereas 20E skewed the brain transcriptome toward a gamergate-like state (Figure 1G).

To test whether these hormone-induced transcriptional changes corresponded to phenotypic alterations, we measured two caste-specific traits: hunting behavior, typical of workers, and reproductive activity, which is restricted to gamergates. We injected hormone analogs with stronger activity and/or stability compared to the natural hormones. The analogs and the corresponding endogenous ligands elicited very similar transcriptional responses (Figure S1E). Consistent with the changes in gene expression, brain injections of the JH3 analog methoprene increased hunting activity (Figures 1H and S1F), whereas brain injections of the 20E analog ponasterone A stimulated ovary activation (Figures 1I, S1G, and S1H). We conclude that JH3 and 20E signaling are sufficient to skew the brain transcriptome toward a worker or gamergate state, respectively, and to stimulate appropriate caste-specific behavior.

JH3 and 20E induce caste-specific transcriptomes *in vitro*

Although our *in vivo* RNA-seq analyses revealed a role for JH3 and 20E in caste-specific gene expression, they could not provide detailed information on the immediate early response to JH3 and 20E, due to the invasiveness of head injections. To define the transcriptional response to these hormones in neurons in a more biochemically controlled setting, we developed primary ant neuronal cultures (Figure 2A). After 6 days in culture, cells isolated from pupal central brains attached and grew projections that were reactive to HRP antibodies (Figures 2B and S2A) (Jan and Jan, 1982). Compared to the frequencies in adult

Please cite this article in press as: Gospocic et al., Kr-h1 maintains distinct caste-specific neurotranscriptomes in response to socially regulated hormones, Cell (2021), https://doi.org/10.1016/j.cell.2021.10.006

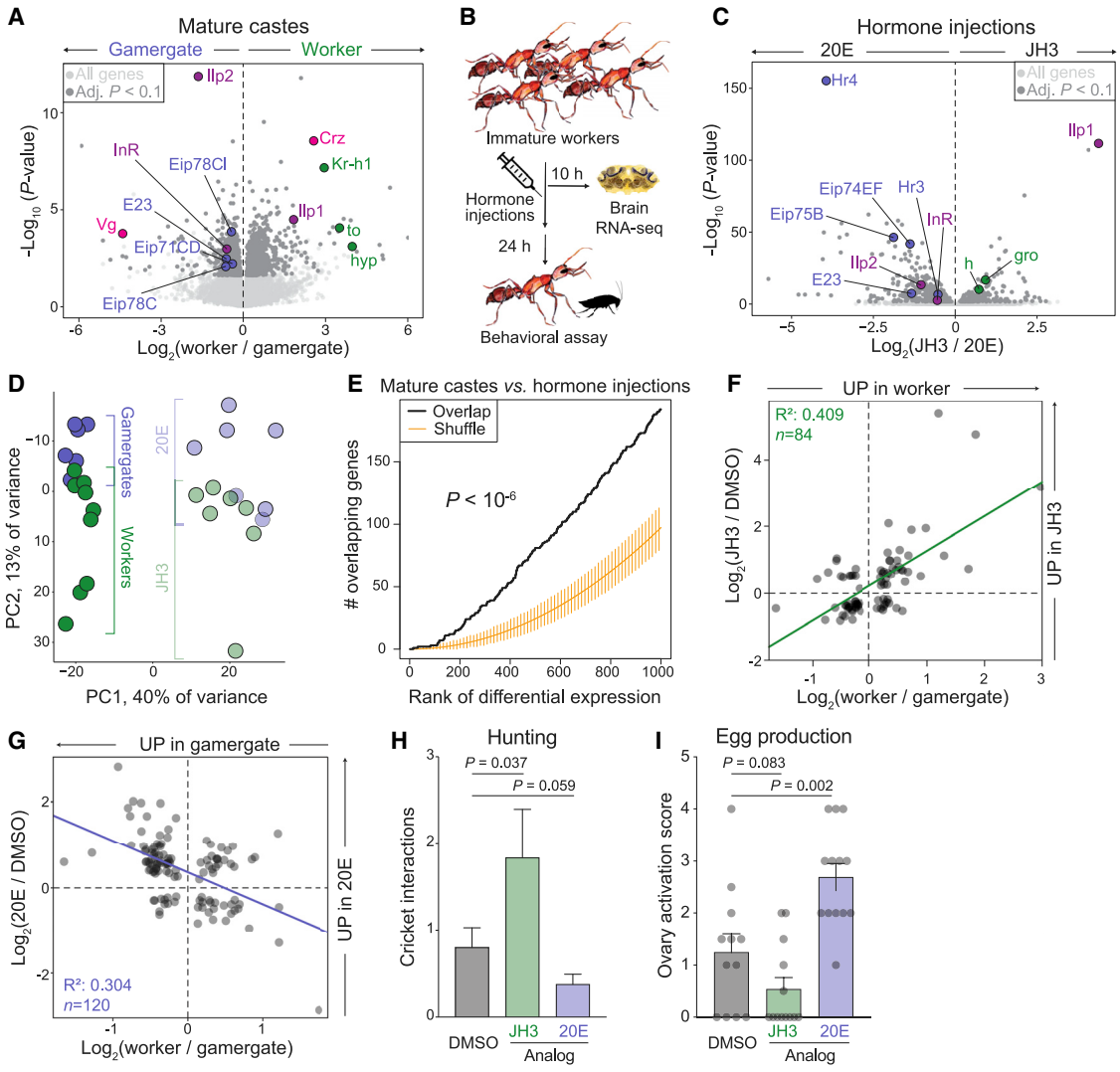

Figure 1. JH3 and 20E drive caste-specific gene expression and behavior

(A) RNA-seq from central brains of mature (4 months old) foraging workers and reproductive gamergates. Genes discussed in the text are highlighted. Data from 9 worker and 5 gamergate brains. Hyp, *hymenoptaecin*.

(B) Experiment scheme. Immature workers were 10 days old.

(C) Brain RNA-seq after injections of JH3 or 20E. Genes referenced in text are in green (JH3) or blue (20E). Data from 7 biological replicates.

(D) PCA based on the 1,000 most variable genes showing mature worker and gamergate brains (full circles) and immature worker brains after JH3 or 20E injections (semi-transparent circles).

(E) Overlap of genes affected by JH3 or 20E injections with those differentially expressed in workers and gamergates (black line). The p value was obtained by comparison with 10^6 random permutations of the gene lists ("shuffle," orange line).

(F and G) Log-fold-changes in genes that responded to JH3 (F) or 20E (G) injections over DMSO (y axis) and worker versus gamergate brains (x axis).

(H) Number of cricket interactions for ants injected with DMSO or hormone analogs in the cricket-in-a-tube assay (Gospocic et al., 2017). Bars represent means + SEM. n = 71, 74, and 74 ants for DMSO, meth (JH3 analog), and ponA (20E analog), respectively. p values are from a generalized linear model based on the negative binomial distribution.

(I) Activation score of ovaries in injected individuals based on the presence of different stages of oocytes and nurse cells. Bars represent the mean + SEM. p values are from ANOVA and Holm-Sidak test.

See also Figure S1 and Tables S1 and S2.

Harpegnathos brains (Sheng et al., 2020), the cultures were enriched for neurons versus glia, as determined by immunofluorescence stainings (Figures 2B, S2B, and S2C) and marker expression analyses (Figures S2D and S2E). Mushroom body (MB) neuron markers were slightly enriched, possibly due to a higher resilience of these neurons to harvesting and *in vitro* culture.

When exposed for 6 days to JH3 or 20E, the neuronal cultures displayed similar morphologies and composition (Figures S2A and S2C), but acquired very distinct transcriptional states, as

Please cite this article in press as: Gospocic et al., Kr-h1 maintains distinct caste-specific neurotranscriptomes in response to socially regulated hormones, Cell (2021), https://doi.org/10.1016/j.cell.2021.10.006

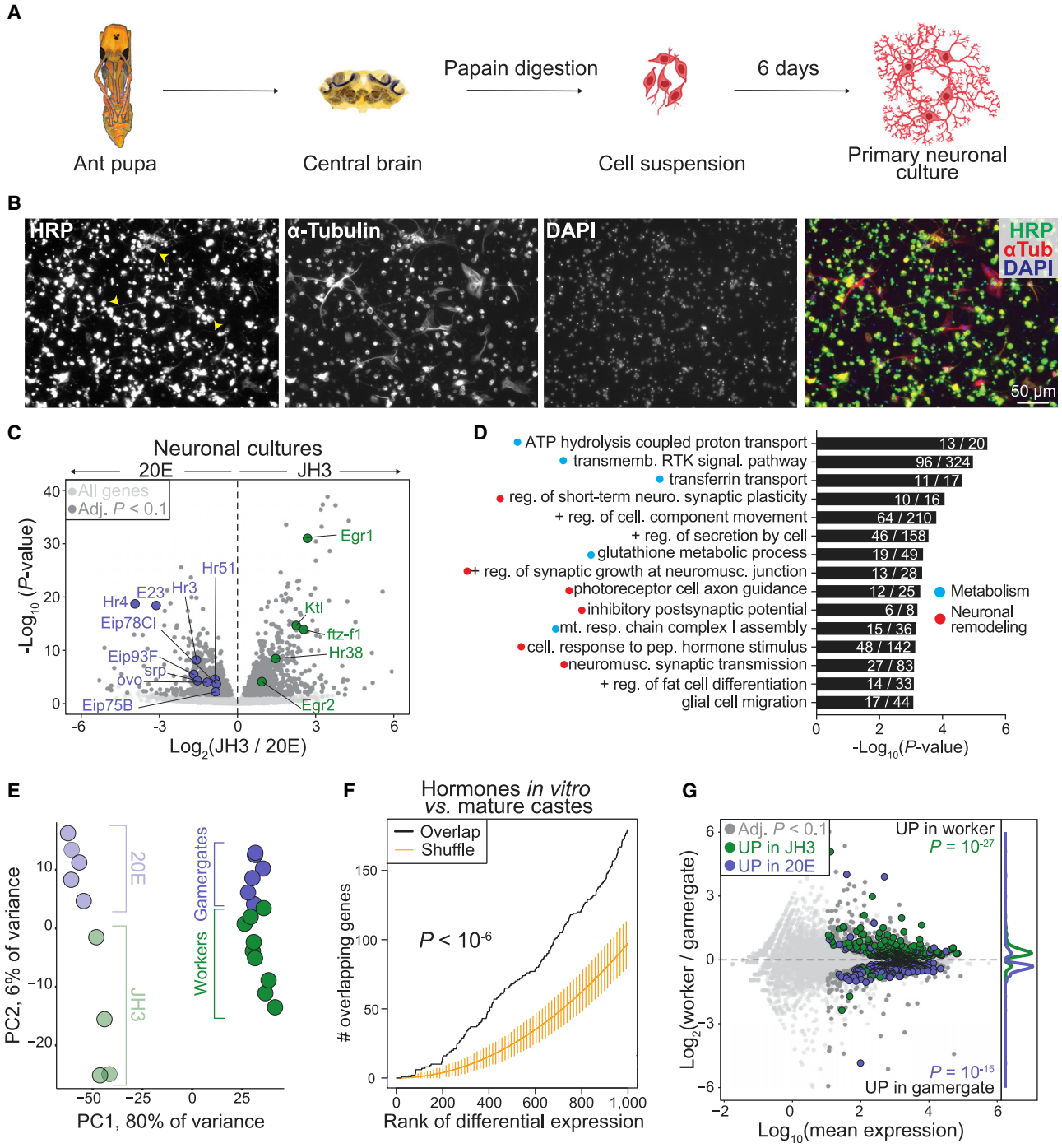

Figure 2. JH3 and 20E recapitulate caste-biased gene expression *in vitro*

(A) Scheme for the preparation of primary neuronal cultures.

(B) Immunofluorescence on neuronal cultures. Arrowheads indicate neuronal projections.

(C) RNA-seq for neuronal cultures maintained in JH3 or 20E conditions. Data are from 4 (JH3) and 5 (20E) biological replicates.

(D) Top "biological process" GO enriched in genes differentially expressed from the JH3 versus 20E comparison in (C).

(E) PCA based on the 1,000 most variable genes for neurons cultured with JH3 or 20E (semi-transparent circles) and brains from mature workers or gamergates (full circles).

(legend continued on next page)

Please cite this article in press as: Gospocic et al., Kr-h1 maintains distinct caste-specific neurotranscriptomes in response to socially regulated hormones, Cell (2021), https://doi.org/10.1016/j.cell.2021.10.006

demonstrated by the differential expression of 2,443 genes (Figure 2C; Table S1). In JH3, the neurons upregulated transcription factors that regulate foraging behavior (*Egr1*, *Egr2*, and *Hr38*), neuronal remodeling (*ftz-f1*), and aggression (*Ktl*) (Boulanger et al., 2011; Singh et al., 2018; Ugajin et al., 2013; Williams et al., 2014) (Figure 2C, green dots), all reminiscent of a worker-like state. Genes upregulated in 20E conditions included ecdysone-responsive genes (*Eip75B*, *Eip78CI*, *Eip93F*, *E23*, *Hr3*, *Hr4*, and *Hr51*) (Figure 2C, blue dots), as well as genes involved in reproduction (*srp* and *ovo*) (Bates et al., 2010; Cáceres et al., 2011; Syed et al., 2017; Uryu et al., 2015), consistent with the reproductive focus of gamergates. In general, genes differentially regulated by JH3 or 20E *in vitro* were enriched for GO terms associated with neuronal remodeling and metabolism (Figure 2D; Table S2).

Similar to our observations with hormone injections *in vivo*, a PCA revealed that the transcriptome of neurons cultured with JH3 bore resemblance to the transcriptome of worker brains, whereas neurons maintained in 20E conditions were more similar to gamergate brains (Figure 2E, PC2). In keeping with this, we observed a significant overlap between genes differentially regulated in neurons cultured in the different hormones and those naturally caste-biased in worker and gamergate brains (Figure 2F). More specifically, genes upregulated in JH3 conditions overlapped with worker genes, whereas genes upregulated in 20E conditions overlapped with gamergate genes (Figure 2G). Although, as would be expected, several genes responded differently to these very different contexts, the remarkable degree of correlation of gene expression *in vitro* and *in vivo* supports the conclusion that the caste-specific brain transcriptomes of *Harpegnathos* workers and gamergates can be partially recapitulated *in vitro* by the presence of JH3 and 20E, respectively.

Correlations between transcriptional signatures of juvenile hormone and ecdysone signaling and caste-biased expression patterns were not exclusive to *Harpegnathos*. We analyzed previously published RNA-seq data from ant species with fixed queen-worker (*Solenopsis invicta* and *Monomorium pharaonis*) or queenless social systems (*Dinoponera quadriceps* and *Ooceraea biroi*). We also analyzed two species of wasps (*Polistes dominula* and *Polistes canadensis*) and bees (*Bombus terrestris* and *Megalopta genalis*) (Chandra et al., 2018; Kapheim et al., 2020; Marshall et al., 2020; Patalano et al., 2015; Standage et al., 2016; Wang et al., 2020). In all cases, genes differentially expressed between non-reproductive and reproductive individuals overlapped significantly with genes regulated by JH3 and 20E in *Harpegnathos* neuronal cultures (Figure S3, Venn diagrams). Furthermore, in all 9 species, genes upregulated by JH3 were preferentially expressed in non-reproductive workers, whereas 20E-responsive genes were preferentially expressed in reproductive individuals (Figure S3, boxplots). Thus, the balance between JH3 and 20E signaling might be a conserved mechanism to establish caste-specific transcriptional states across Hymenoptera.

JH3 and 20E affect overlapping neuronal populations

Although the strong dichotomy in the transcriptional response to JH3 and 20E suggests a global shift in gene expression across various neuronal types in the brain, it could also be that distinct small populations of JH3- or 20E-reactive neurons are responsible for the observed changes in bulk gene expression.

We re-analyzed single-cell RNA-seq data from worker and gamergate brains (Sheng et al., 2020) (Figures S4A and S4B) and determined the expression bias of JH3- and 20E-sensitive genes in single cells. Two thirds of all neurons displayed a skew in gene expression consistent with JH3-dependent activation in workers (Figures S4C, top, and S4D). Typically, the same cell types also displayed 20E-associated transcriptional profiles in gamergates (Figures S4C, bottom, and S4E). An exception was found in a small cluster of excitatory clock neurons expressing *Gadd45* and *Lsd-2* (Figure S4F), which have been implicated in regulation of oviposition and energy homeostasis (Plyusnina et al., 2011; Thimgan et al., 2010), and displayed gamergate-biased expression of some JH3-responsive genes. Thus, our single-cell analyses confirmed the JH3 and 20E signaling dichotomy in worker and gamergate brains and suggested that broadly overlapping neuronal populations acquire distinct transcriptional states in response to these hormones.

Kr-h1 is induced by both JH3 and 20E

Once bound by their ligand, steroid hormone receptors activate target genes, which often include many transcription factors, transforming the internal cell state through changes in metabolism, synaptic potentiation, and transcription (Gray et al., 2017; Koyama et al., 2020; Yaniv and Schuldiner, 2016). To define the plastic response of the neuronal transcriptome to socially regulated hormonal changes, we simulated the effects of caste transitions by switching neurons grown in JH3 to 20E (mimicking a worker-gamergate "forward" transition) and neurons grown in 20E to JH3 (mimicking a gamergate-worker "reverse" transition) and profiled gene expression after 30 min, 6 h, and 24 h (Figure 3A; Table S1).

We focused on genes encoding transcription factors that were upregulated in response to acute treatment with JH3 or 20E (Figures 3B and 3C), although a small number of downregulated genes was also detected (Figures S2F and S2G). Several of the transcription factors induced by JH3 and 20E *in vitro* were also differentially expressed between worker and gamergate brains *in vivo* (Figures 3B and 3C, blue and green dots). Consistent with the notion that JH3 and 20E promote diverging transcriptional programs that correlate with separate caste identities, the list of transcription factors activated during the forward and reverse hormonal switch *in vitro* were largely distinct (Figure 3D). However, five transcription factors were induced by both

(F) Overlap of genes differentially expressed between neurons grown in JH3 and 20E with caste-biased genes from Figure 1. The p value was obtained by comparison with 10^6 random permutations.

(G) The MA plot shows differential gene expression in mature worker and gamergate brains (from Figure 1A). Colors highlight the genes upregulated (adj. $p < 0.1$) in neurons grown in JH3 (green) or 20E (blue) conditions *in vitro*. p values are from Fisher's exact tests for the overlaps of the significant genes *in vitro* and *in vivo*. See also Figures S2, S3, and S4 and Tables S1 and S2.

Please cite this article in press as: Gospocic et al., Kr-h1 maintains distinct caste-specific neurotranscriptomes in response to socially regulated hormones, Cell (2021), https://doi.org/10.1016/j.cell.2021.10.006

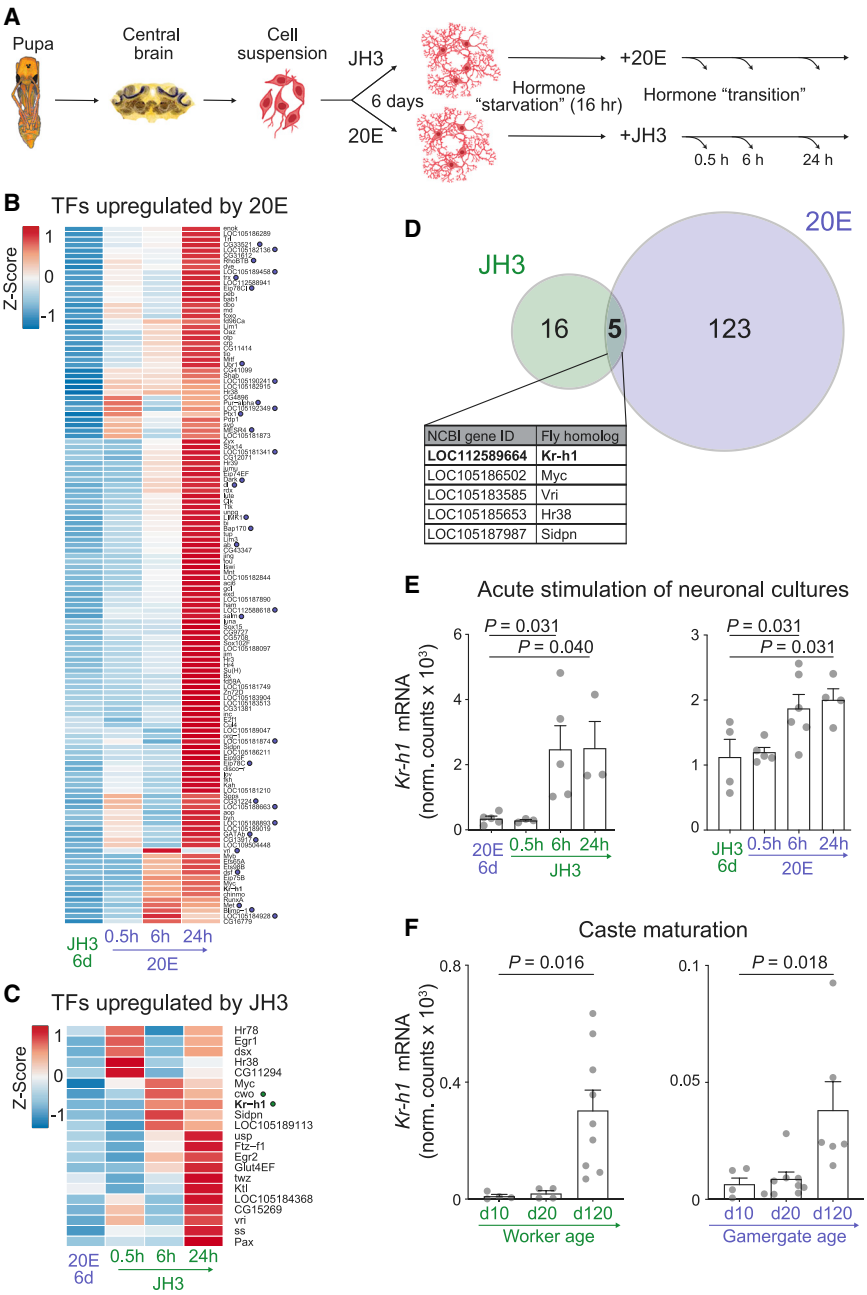

Figure 3. Kr-h1 is induced by JH3 and 20E

(A) Experiment scheme.

(B and C) Heatmaps for the expression levels (DESeq2-normalized counts) of transcription factors induced by 20E (B) or JH3 (C) in at least one time point (adj. $p < 0.1$). Genes differentially expressed in gamergates (B) or workers (C) are indicated with blue or green dots, respectively. Data from ≥ 4 biological replicates.

(D) Overlap of transcription factors induced by 20E and JH3 from (B) and (C).

(E and F) Expression levels (DESeq2-normalized counts) of *Kr-h1* after JH3 or 20E stimulation of neuronal cultures (E) or in the brain of maturing workers and gamergates (F). Bars represent mean + SEM. p values are from one-way ANOVA and Holm-Sidak tests.

See also Figure S2 and Table S1.

hormonal transitions at one or more time points. Of these, only *Kr-h1* was induced as early as 6 h and remained at higher levels at 24 h in both treatments (Figure 3E).

We turned our attention to *Kr-h1* because of its connections with social behavior and hormone signaling, as well as its potential role in neuronal remodeling (Shi et al., 2007). Kr-h1 is a zinc finger transcription factor that responds to juvenile hormone (Lozano and Belles, 2011; Minakuchi et al., 2008, 2009; Ojani et al., 2018) and to social stimuli in the honeybee brain, where it is upregulated during the transition from nursing to foraging behavior (Fussnecker and Grozinger, 2008; Grozinger and Robinson, 2007; Grozinger et al., 2003). Consistent with this, we detected the upregulation of *Kr-h1* in aging *Harpegnathos* workers as they transition from "inside" colony tasks to foraging (Figure 3F, left), However, we unexpectedly also observed increasing levels of *Kr-h1* transcripts in the brain of maturing gamergates (Figure 3F, right), suggesting that *Kr-h1* becomes upregulated over time as individuals become firmly established in their social castes.

Kr-h1 represses distinct genes in workers and gamergates

We were intrigued by the fact that Kr-h1 was upregulated *in vitro* in response to both JH3 and 20E, which promote worker and gamergate identity, respectively. We reasoned that if a single transcription factor contributes to different caste-specific transcriptomes, it must be able to bind and regulate different sets of genes in different conditions. We performed Kr-h1 chromatin immunoprecipitation sequencing (ChIP-seq) from brains of workers and gamergates using a custom antibody (Figure S5A). Kr-h1 was bound predominantly to genic regions, in particular promoters (Figure 4A). In total, 5,981 genes possessed a strong (fold-over-input >3) Kr-h1 peak at the promoter or within the gene body. Among the GO terms that were associated with genes bound by Kr-h1, some were related to neuronal remodeling and caste-specific processes, such as "*axon guidance*," "*oogenesis*," and "*insulin receptor signaling*" (Figure S5B; Table S2).

Genomic regions bound by Kr-h1 were significantly enriched (p value = 5.5×10^{-56}, Fisher's exact test) for genes differentially expressed in workers and gamergates (Figure 4B). For example, we observed higher Kr-h1 binding in gamergates compared to workers at the *corazonin* (*Crz*) locus, which encodes a

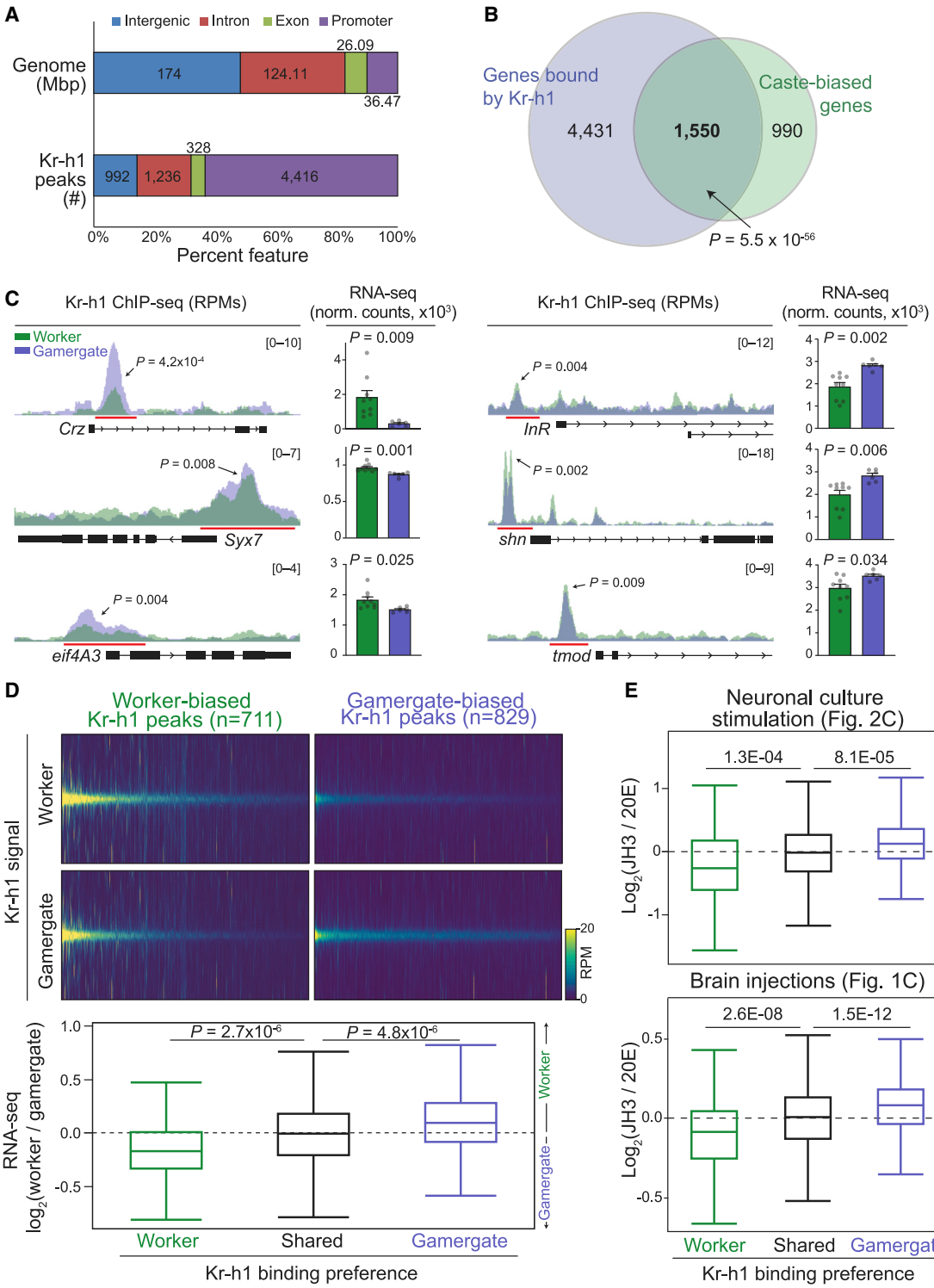

Figure 4. Kr-h1 binds to caste-biased genes

(A) Proportion of Kr-h1 peaks (fold over input >3) within genomic features. For global peak distribution, data from worker and gamergate brains were combined.

(B) Overlap of genes bound by Kr-h1 and differentially expressed between workers and gamergates (Figure 1A). p value is from a Fisher's exact test.

(C) Tracks for Kr-h1 occupancy in mature worker and gamergate brains. p values are from DiffBind. To the right are expression levels (DESeq2-normalized counts). Bars represent the mean + SEM. p values are from Student's t tests. ChIP-seq data are from 5 biological replicates per caste. RPM, reads per million.

(legend continued on next page)

neuropeptide preferentially expressed in worker brains (Gospocic et al., 2017) (Figure 4C, top left). Other genes with stronger Kr-h1 binding in gamergates included *Syx7*, which encodes a protein involved in the synaptic vesicle cycle and neurotransmitter release, and *eif4A3*, both of which were expressed at higher levels in workers (Figure 4C, left). Conversely, the gene for the insulin receptor, *InR*, as well as *shn* and *tmod*, were preferentially bound by Kr-h1 in workers and expressed at higher levels in gamergates (Figure 4C, right).

Beyond these examples, Kr-h1 occupancy and gene expression were anti-correlated in a caste-dependent manner genome-wide. We identified 711 and 829 genomic regions with significantly ($p < 0.01$, Wald negative binomial test) higher Kr-h1 occupancy in brain chromatin from workers or gamergates, respectively (Figure 4D, top). Genes with caste differences in Kr-h1 binding were enriched for GO terms related to transcriptional and epigenetic regulation as well as neuronal remodeling (Figure S5C; Table S2). Genome-wide, genes bound by Kr-h1 in workers were expressed at higher levels in gamergates and vice versa (Figure 4D, bottom), suggesting that Kr-h1 maintains caste-specific transcriptomes by repressing genes for the opposite caste.

Genes with a caste-biased occupancy of Kr-h1 were also differentially sensitive to JH3 and 20E: genes preferentially bound by Kr-h1 in worker brains were repressed in response to JH3 and genes preferentially bound by Kr-h1 in gamergate brains were repressed in response to 20E both *in vitro* (Figure 4E, top) and *in vivo* (Figure 4E, bottom). Similar to what we had observed for the transcriptional response to JH3 and 20E, genes with preferential Kr-h1 binding in workers or gamergates were differentially expressed in multiple populations of neurons across castes (Figures S5D and S5F), excluding the possibility that small subsets of neurons might be responsible for the genome-wide differences.

Overall, our data show that Kr-h1 binds to distinct sets of caste-biased genes in worker and gamergate brains and that these genes are preferentially repressed in response to JH3 and 20E, respectively.

Kr-h1 maintains transcriptional caste boundaries

To demonstrate that Kr-h1 maintains caste-specific expression profiles in the brain, we injected short interfering RNAs (siRNAs) against Kr-h1 into the heads of immature (day 10) workers, as well as age-matched individuals in the early phase of the transition to gamergate (“immature gamergates”). Ten hours after injection, we observed efficient depletion of *Kr-h1* mRNA (Figure 5A) and extensive downstream transcriptional responses in both castes, with 569 differentially expressed genes in immature workers and 2,052 in immature gamergates (Figure 5B).

Our ChIP-seq and RNA-seq analyses in mature workers and gamergates (Figure 4) suggested that Kr-h1 functions as a caste-specific transcriptional repressor in the *Harpegnathos* brain. Consistent with this notion, depletion of Kr-h1 in immature workers or gamergates resulted in the de-repression of genes bound by Kr-h1 in the respective caste (Figure 5B). A quantitative analysis confirmed that the set of worker-biased Kr-h1 targets became significantly more active when Kr-h1 was depleted in workers, and vice versa for gamergate-biased targets (Figure 5C). In each case, the opposite set of caste-specific targets became less active upon knockdown, possibly due to indirect effects and feedback loops. Based on these and our previous observations, we reasoned that Kr-h1 might be functionally required in each caste to repress the transcriptional program of the opposing caste. Indeed, genes displaying gamergate-biased expression in mature castes (from Figure 1A) were preferentially upregulated in response to Kr-h1 knockdown in immature workers and, conversely, worker-biased genes were activated when Kr-h1 was depleted in immature gamergates (Figures 5D and S6A).

Among the genes upregulated after Kr-h1 knockdown, we found several that exhibited differential expression in mature castes and differential responses to hormonal treatments *in vitro* and *in vivo*, including *Syx7* and *eif4A3*, which were repressed by Kr-h1 in gamergates and induced by JH3 (Figure 5E), as well as *InR* and *tmod*, which were repressed by Kr-h1 in workers and induced by 20E (Figure 5F). Consistent trends were observed for *Crz* and *shn* (Figure S6B), although in these cases the effects did not reach statistical significance. At a broader level, we detected significant overlaps of the genes affected by Kr-h1 knockdowns in immature workers or gamergates with genes differentially expressed in the mature castes, differentially bound by Kr-h1, and differentially sensitive to JH3 or 20E stimulation *in vivo* and *in vitro* (Figure S6C). These results indicate that Kr-h1 is a major player in the maintenance of caste-specific transcriptomes in *Harpegnathos* brains.

Kr-h1 regulates caste phenotype

Based on our observations of caste-specific transcriptional regulation by Kr-h1, we reasoned that its loss might result in distinct phenotypic outcomes in the two castes. Consistent with the proposed role for Kr-h1 in foraging of worker bees (Fussnecker and Grozinger, 2008; Grozinger and Robinson, 2007), knocking it down in the brain of immature *Harpegnathos* workers inhibited hunting (Figures 6A and 6B, green bars, and S7A, left). This effect was exquisitely caste-specific: depletion of Kr-h1 in immature gamergates had the opposite outcome (Figures 6B, blue bars, and S7A, right). Thus, Kr-h1 maintains normal patterns of hunting behavior by promoting it in workers and suppressing it in gamergates.

To determine whether Kr-h1 has caste-specific roles also in the context of reproductive activity, we performed RNA-seq on the ovaries of mature workers or gamergates after Kr-h1 knockdown in their brains. As expected from their different functional status, 7,014 genes were differentially expressed in ovaries from control mature workers versus gamergates, including

(D) Top: heatmap for Kr-h1 ChIP-seq at differentially bound regions ±1 kb. Bottom: differential expression in worker versus gamergate brains for genes differentially bound by Kr-h1. p values are from Mann-Whitney U tests.
(E) Same as (D) but showing differential expression in response to JH3 versus 20E *in vitro* (top) or *in vivo* (bottom).
See also Figure S5 and Table S2.

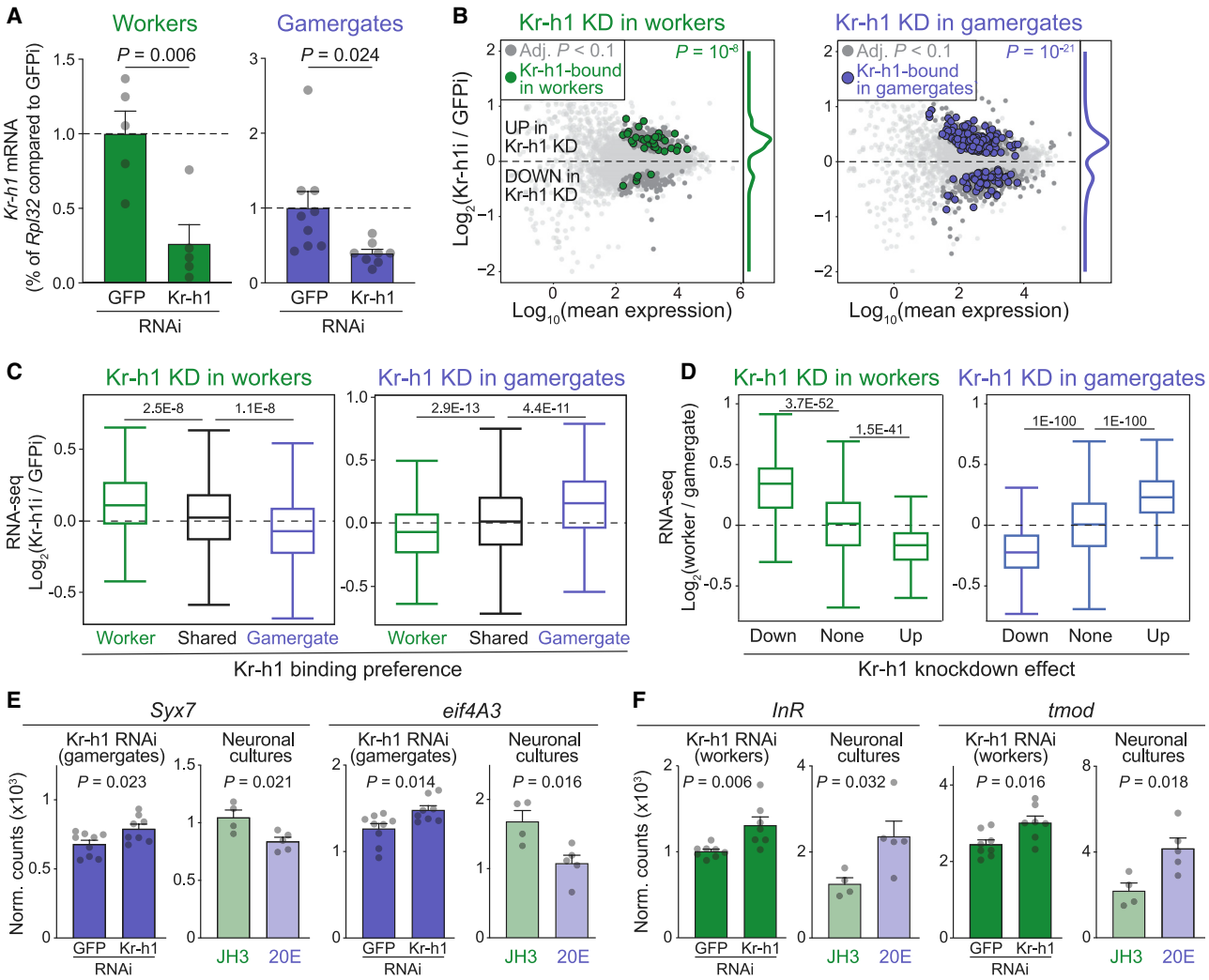

Figure 5. Kr-h1 represses caste-inappropriate genes

(A) RT-qPCR for Kr-h1 in the brains of immature workers (left) or gamergates (right) injected with siRNAs against Kr-h1 or GFP. Data are normalized to the housekeeping gene *Rpl32* and shown as the ratio to the GFPi control. Bars represent the mean + SEM. p values are from Student's t tests.

(B) The MA plots show differential expression upon Kr-h1 knockdown in immature workers or gamergates. Colors highlight genes with caste-biased Kr-h1 binding in workers (left, green) or gamergates (right, blue). p values are from Fisher's exact tests for the gene set overlaps.

(C) Differential expression upon Kr-h1 knockdown in immature workers (left) or gamergates (right). Genes were classified according to their Kr-h1 binding preference in the brains of the mature castes as in Figures 4D and 4E. p values are from Mann-Whitney U tests.

(D) Differential expression in mature workers and gamergates. Genes were classified according to the effect of Kr-h1 knockdown in immature workers (left) or gamergates (right). p values are from Mann Whitney U tests.

(E and F) Expression levels (DESeq2-normalized counts) after Kr-h1 knockdown and in neuronal cultures. Bars represent mean + SEM. p values are from Student's t tests.

See also Figure S6 and Table S1.

markers of cell proliferation and ovary activation *aurA*, *fs(1)Ya*, and *cort* (Blengini et al., 2021; Chu et al., 2001; Lin and Wolfner, 1991), which were greatly upregulated in gamergates (Figure S7B, red; Table S1). Loss of Kr-h1 in the brain resulted in 559 significantly affected genes in the ovaries of mature workers and 2,751 in the ovaries of mature gamergates (Figure 6C). Among genes that became upregulated in workers, some were potentially involved in oocyte maturation (e.g., *CycB*, *osk*, and *Tre1*) (Flora et al., 2018; Kim-Ha et al., 1991; Kunwar et al., 2003) and ecdysone biosynthesis (*sro* and *dib*) (Niwa et al., 2010; Warren et al., 2002) (Figure 6C, left), which was reflected in the enrichment of related GO terms such as "*ecdysone biosynthetic process*" and "*female meiotic nuclear division*" (Table S2). In contrast, Kr-h1 knockdown in the brain of mature gamergates induced ovary expression of genes annotated as positive regulators of autophagy (e.g., *Sesn*, *shi*, *Synj*, *Lerp*, and *sima*), including multiple autophagy-related (ATG) genes (*Atg14*, *Atg17*, and *Atg101*) (Figure 6C, right), suggestive of ovary

Please cite this article in press as: Gospocic et al., Kr-h1 maintains distinct caste-specific neurotranscriptomes in response to socially regulated hormones, Cell (2021), https://doi.org/10.1016/j.cell.2021.10.006

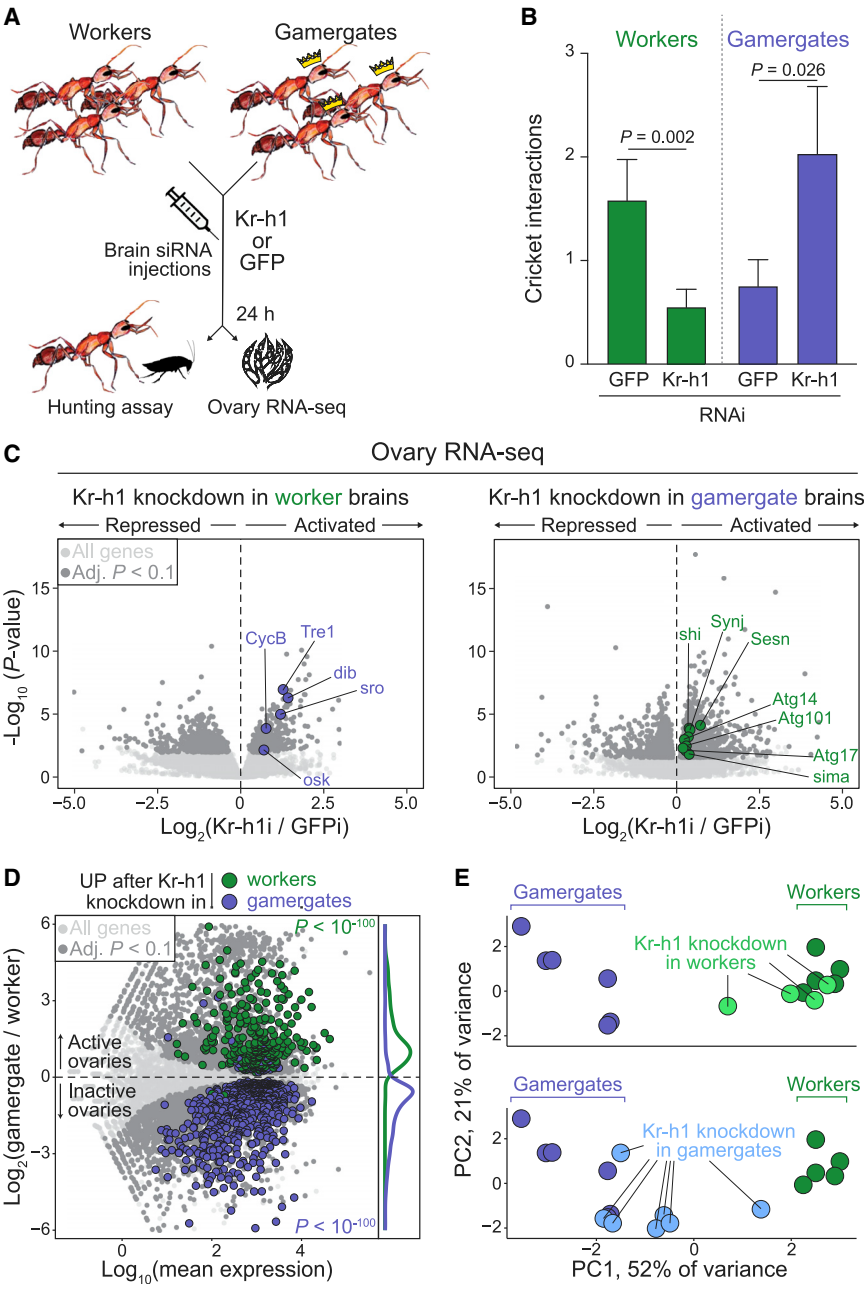

Figure 6. Kr-h1 stabilizes caste identity

(A) Experiment scheme. The hunting assay was performed in immature workers or gamergates (10 days old). For ovary RNA-seq, the knockdowns were performed in mature individuals (4 months old).

(B) Interactions with crickets trapped in a tube (Gospocic et al., 2017). Bars represent mean + SEM. p values are from a generalized linear model based on the negative binomial distribution.

(C) RNA-seq from ovaries after Kr-h1 knockdown in the brain of mature workers (left) or gamergates (right). Data are from 5 (worker GFPi), 4 (worker Kr-h1i), 6 (gamergate GFPi), and 7 (gamergate Kr-h1i) replicates.

(D) The MA plot shows differential gene expression in control mature worker and gamergate ovaries. Colors highlight genes derepressed in the ovaries after Kr-h1 knockdown in mature workers (green) or gamergates (blue). p values are from Fisher's exact tests for the overlaps.

(E) PCA based on the 2,000 most variable genes in control workers and gamergates. Ovary transcriptomes of mature workers (green) and gamergates (blue) after GFP RNAi were compared to ovaries after Kr-h1 RNAi in the brain of mature workers (top) or gamergates (bottom).

See also Figure S7 and Tables S1 and S2.

function shutdown (Fang et al., 2016; Hasanagic et al., 2015; Lee et al., 2010; Löw et al., 2013; Vanhauwaert et al., 2017).

Genome-wide, brain Kr-h1 knockdowns caused caste-dependent changes in ovary gene expression: genes upregulated in worker ovaries after brain knockdown of Kr-h1 overlapped with genes normally expressed in active gamergate ovaries (Figure 6D, green dots), whereas genes upregulated in gamergate ovaries after Kr-h1 knockdown were expressed at higher levels in the inactive ovaries of control workers (Figure 6D, blue dots). Overall, Kr-h1 knockdown in the brain shifted the transcriptome of worker ovaries toward that of gamergates (Figure 6E, top) and vice versa (Figure 6E, bottom). Thus, also in the context of a gamergate-specific phenotypic trait—reproductive activity—the role of Kr-h1 is to maintain the *status quo*, i.e., ovary activation in gamergates and ovary suppression in workers.

Kr-h1 connects hormonal signaling to caste-specific gene regulation

To establish a link between caste-specific hormones, Kr-h1 binding, and gene expression, we performed ChIP-seq in *Harpegnathos* brains for the JH3 and 20E nuclear receptors, Met and EcR, using custom antibodies (Figure S7C). The receptors localized predominantly to gene promoters (Figure S7D), as expected from their role in transcriptional regulation. We found extensive overlap for Met and Kr-h1 binding sites on chromatin (Figure 7A, top) and, unexpectedly, between EcR and Kr-h1 as well (Figure 7A, bottom). In fact, a large majority (~90%) of genes bound by Met also contained peaks for both EcR and Kr-h1 (Figure S7E). Further, Met and EcR binding sites were greatly enriched ($p < 10^{-100}$, Fisher's exact test) at caste-biased genes that also contained a Kr-h1 binding site (Figure 7B, Kr-h1^{+}), but not at caste-biased genes devoid of Kr-h1 (Figure 7C, Kr-h1^{-}). Genes bound by Met were enriched for worker-biased genes (Figure 7D, left), whereas genes bound exclusively by EcR and not by Met (EcR^{+}/Met^{-}) were more likely to be gamergate-biased (Figure 7D, right).

Please cite this article in press as: Gospocic et al., Kr-h1 maintains distinct caste-specific neurotranscriptomes in response to socially regulated hormones, Cell (2021), https://doi.org/10.1016/j.cell.2021.10.006

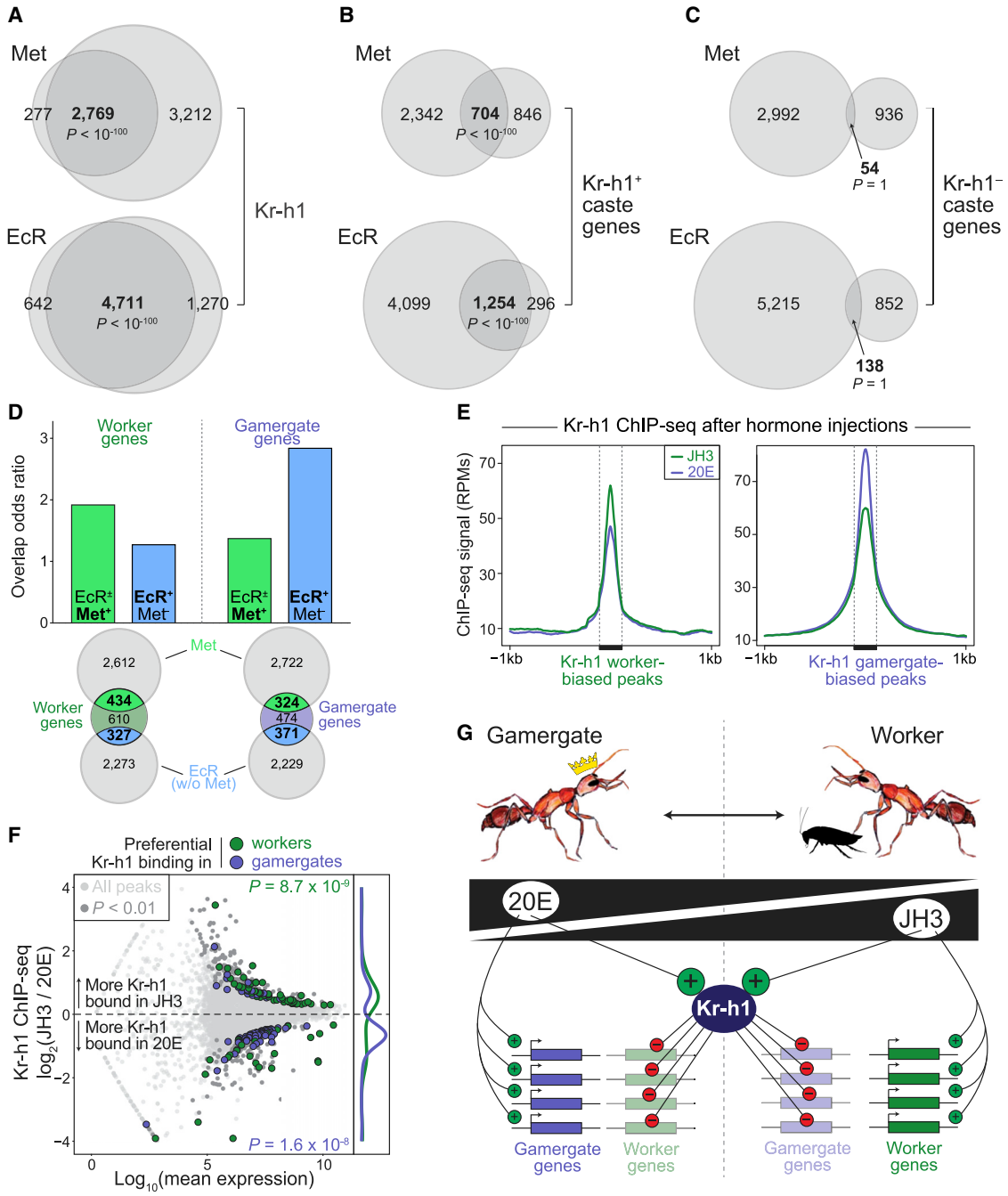

Figure 7. JH3 and 20E regulate the genomic distribution of Kr-h1

(A–C) Overlap of genes with peaks for Met (top), EcR (bottom), and Kr-h1 (A), genes with caste-biased expression and bound (B) or not (C) by Kr-h1. Data are from 6 replicates (3 workers and 3 gamergates) for both Met and EcR. For peak determination worker and gamergate data were combined. Kr-h1 peaks are from Figure 4. p values are from Fisher's exact tests.

(D) Overlap of genes bound by Met (light green) or genes bound by EcR without Met (light blue) with worker-biased (left) or gamergate-biased (right) genes. Top: odds ratios for the overlaps. Bottom: number of overlapping genes in each category.

(E) Metaplots for Kr-h1 occupancy (RPMs) on the top 500 differentially bound regions across castes ±1 kb after head injections of JH3 (green) or 20E (blue). Data are from 2 biological replicates (injections) per condition.

(F) The ChIP-seq MA plot shows differential binding of Kr-h1 after injection of JH3 or 20E, as in (E). Colors highlight peaks with more Kr-h1 bound in workers (green) or gamergates (blue). p values are from Fisher's exact tests for the overlaps.

(G) Proposed model.

See also Figure S7.

Please cite this article in press as: Gospocic et al., Kr-h1 maintains distinct caste-specific neurotranscriptomes in response to socially regulated hormones, Cell (2021), https://doi.org/10.1016/j.cell.2021.10.006

Based on this extensive co-localization, we hypothesized that JH3 and 20E signaling might be sufficient to direct Kr-h1 to caste-specific targets on chromatin. Indeed, brain injection of JH3 resulted in increased binding to worker-specific Kr-h1 targets (Figures 7E, left, and 7F, green dots), whereas injection of 20E resulted in the redistribution of Kr-h1 in the opposite direction, with increased occupancy of target genes normally bound in gamergates (Figures 7E, right, and 7F, blue dots).

Together, our data support a model (Figure 7G) by which Kr-h1 binds to and regulates different target genes in workers and gamergates in response to JH3 and 20E. In workers, Kr-h1 represses genes typically expressed at higher levels in gamergates, whereas in gamergates, it represses worker-biased genes. The result of this caste-specific repressive activity of Kr-h1 is a reinforcement of the transcriptional boundaries between social castes.

DISCUSSION

We utilized a plastic caste system to explore the mechanism by which hormonal signaling establishes distinct brain states and how these states are maintained to give rise to stable social castes. In *Harpegnathos*, workers and gamergates exhibit distinct behavioral repertoires that likely originate from caste-specific gene regulation. By analyzing the transcriptional and behavioral response to JH3 and 20E *in vivo* and *in vitro*, we conclude that these two hormones are key to the caste identities of workers and gamergates and that Kr-h1 is required to maintain the transcriptional boundaries that separate these two brain states.

Hormonal regulation of caste-specific transcriptional states

We identified a striking dichotomy between the two hormonal pathways and the social castes: the worker transcriptome was dominated by JH3-induced genes, whereas gamergates showed a 20E-dependent gene expression signature (Figure 1). These observations are consistent with studies that reported different levels of juvenile hormones and ecdysteroids in castes of several social insects (Bloch et al., 2000; Brent et al., 2006; Brian, 1974; Rachinsky et al., 1990; Robinson et al., 1991; Wheeler and Nijhout, 1981) and a correlation between increased levels of JH3 and the age-associated transition to foraging in honeybees and ants (Dolezal et al., 2012; Elekonich et al., 2001; Huang et al., 1991). Here, we directly demonstrated that activation of JH3 and 20E signaling in the brain stimulated worker behavior and reproductive activity, respectively (Figure 1). This result confirms and extends the finding of a previous report, whereby long-term systemic administration of methoprene or 20E by feeding was shown to affect *Harpegnathos* ovary development (Opachaloemphan et al., 2021). Echoes of the dichotomy between JH3- and 20E-driven transcriptomes could be observed in several Hymenoptera species (Figure S3), supporting a role for juvenile hormones and ecdysteroids in the evolution of caste systems in social insects. We note, however, that although our results indicate that JH3 and 20E are sufficient to drive portions of the caste-specific transcriptomes, proof of their necessity to caste determination and caste transitions in *Harpegnathos* awaits the development of the appropriate genetic tools.

In mammals, steroid hormone receptors act as master regulators by binding to and activating genes encoding a variety of transcription factors, which in turn regulate hundreds or thousands of downstream genes (Gray et al., 2017; Ogawa et al., 2020). In *Harpegnathos* neurons, the first wave of genes activated in response to JH3 included transcription factors such as *ftz-f1*, required for the establishment of caste-specific transcriptomes in *Apis mellifera* (Mello et al., 2019); and *Hr38*, which is upregulated in the brains of foraging honeybees compared to nurses (Yamazaki et al., 2006). Several transcription factors responded to 20E stimulation, including the only known insect receptor for nitric oxide (NO), *Eip75B* (Brenman et al., 1996; Rabinovich et al., 2016; Reinking et al., 2005; Sunico et al., 2005). NO signaling regulates aggression in mice and territorial fighting among field crickets (Nelson et al., 1995; Stevenson and Rillich, 2015). Given the importance of social conflict in promoting the worker-gamergate transition via the dueling tournament, it is tempting to speculate that 20E might contribute to the establishment of the social hierarchy in *Harpegnathos* by regulating the NO pathway.

Although, in general, the transcription factors activated by JH3 or 20E *in vitro* were different, a few were induced by both (Figure 3). Among these few was Kr-h1, a known effector of juvenile hormone (Jindra et al., 2013) that had not previously been linked to ecdysone. Our findings in *Harpegnathos* place Kr-h1 downstream of both JH3 and 20E signaling and as a crucial regulator of transcriptional identity in both workers and gamergates.

Kr-h1 and the maintenance of social boundaries

We profiled the genomic distribution of Kr-h1 and found that changes in Kr-h1 binding on brain chromatin between workers and gamergates were strongly associated with changes in gene expression, whereby Kr-h1 occupancy correlated with repression (Figure 4). In flies, Kr-h1 associates with a histone deacetylase complex, Sin3-HDAC, required for the maintenance of neuronal identity (Huang et al., 1999; Rhee et al., 2014), suggesting the possibility that repression of transcription by Kr-h1 occurs via changes to chromatin structure. This mechanism would be in keeping with the important role for histone acetylation in regulating caste-biased gene expression in the brain of the ant *Camponotus floridanus* (Glastad et al., 2020; Simola et al., 2016).

Consistent with its caste-specific patterns of chromatin binding, knockdown of Kr-h1 in the brain of workers and gamergates had distinct outcomes: loss of Kr-h1 in immature workers stimulated expression of gamergate-biased genes and, vice versa, loss of Kr-h1 in immature gamergates led to the upregulation of worker-biased genes (Figure 5). Remarkably, the contributions of Kr-h1 to social behavior were also caste-specific (Figure 6): knockdown of Kr-h1 in workers inhibited hunting, whereas the same treatment in gamergates promoted this behavior, which is typically associated with the worker caste. Based on these observations, we conclude that Kr-h1 maintains caste boundaries by repressing "socially inappropriate" patterns of gene expression in the brain (Figure 7G).

Mechanism of Kr-h1 regulation

We propose that Kr-h1 reinforces and maintains JH3- and 20E-induced gene signatures through chromatin-based mechanisms.

Acute administration of JH3 and 20E in the brain resulted in the rapid redistribution of Kr-h1 to its natural target sites in mature workers and gamergates, respectively (Figures 7E and 7F), suggesting the existence of a direct, mechanistic link between hormone signaling and Kr-h1 localization.

One open question is how the same transcription factor, Kr-h1, acquires distinct caste-specific profiles on chromatin depending on social status. A possibility is that JH3 and 20E induce different Kr-h1 isoforms. This idea is supported by observations in *Drosophila*, where two Kr-h1 isoforms are differentially regulated during pupal development and this isoform switch coincides with changes in JH3 and 20E titers (Pecasse et al., 2000; Schuh et al., 1986; Shi et al., 2007). A detailed analysis of our RNA-seq data revealed a small but significant difference in *Kr-h1* exon usage in the brains of workers and gamergates (Figure S7F). Additional experiments are needed to determine whether these two transcriptional isoforms of Kr-h1 regulate caste-specific transcription and behavior.

A second possibility is that selection of Kr-h1 targets depends on Kr-h1-interacting proteins. These need not be mutually exclusive, because alternative Kr-h1 isoforms may form different repressive complexes with distinct target genes. Promising candidates for factors that might recruit Kr-h1 to different genes are the JH3 and 20E nuclear receptors, Met and EcR. Our data show that these receptors extensively co-localize with Kr-h1 on chromatin at loci encoding genes differentially regulated between castes (Figures 7A–7C). However, the presence of Met at ~50% of EcR-bound genes excludes a simple model whereby Met recruits Kr-h1 to its worker-specific targets and EcR recruits it to gamergate-specific targets. The biochemical details of the interplay between Met, EcR, and Kr-h1 in *Harpegnathos* will require additional work to be uncovered and are likely to reveal important aspects of the molecular regulation of social status in ants and beyond.

Conclusions and outlook

Our data indicate that Kr-h1 is a core transcriptional regulator of caste identity. In gamergates, Kr-h1 is downstream of 20E signaling and is involved in maintaining gamergate identity through repression of worker-biased genes. In workers, Kr-h1 is induced by JH3 and downregulates gamergate-biased genes. Given the conservation of JH3 and 20E gene expression signatures, we speculate that the role of Kr-h1 in caste maintenance might also be conserved in other social insects. Future studies will be needed to fully elucidate how JH3 and 20E control caste behavior via Kr-h1 in *Harpegnathos* and to what extent these mechanisms might affect social behavior and brain plasticity in other animals.

Limitations of study

The effects on gene expression, behavior, and ovary status observed upon Kr-h1 knockdown were of lower magnitude compared to the effects of injecting hormones or hormone analogs. Although it is possible that different treatment kinetics might be responsible for these differences, we consider it more likely that Kr-h1 is only one of multiple factors that shape the transcriptional response to JH3 and 20E in the brain. Regarding behavioral quantification, the cricket-in-the-tube assay has some limitations, including the fact that a considerable fraction of the ants from both immature castes did not hunt at all. Although this was taken into account by our statistical analyses, additional assays should be developed to bring further insights on the molecular regulation of behavioral plasticity. Finally, our manipulations in the current study were limited to *Harpegnathos* ants. Until our observations are confirmed in other social and solitary insects, any generalization advanced in our discussion must be considered speculative.

STAR★METHODS

Detailed methods are provided in the online version of this paper and include the following:

- KEY RESOURCES TABLE
- RESOURCE AVAILABILITY
  - Lead contact
  - Materials availability
  - Data and code availability
- EXPERIMENTAL MODEL AND SUBJECT DETAILS
  - Harpegnathos husbandry and worker-gamergate transitions
  - Ant neuronal cell cultures
  - Preparation of honeybee pupal extract for *in vitro* cultures
- METHOD DETAILS
  - Brain dissections
  - RNA isolation and sequencing
  - Hormone injections
  - Hunting assay
  - Ovary imaging and quantification
  - Immunofluorescence on neuronal cultures
  - Hormonal stimulation of neuronal cultures
  - Custom antibody production
  - ChIP-sequencing
  - RNAi for Kr-h1
  - RT-qPCR for Kr-h1
- QUANTIFICATION AND STATISTICAL ANALYSIS
  - Assignment of gene homology and functional terms
  - RNA-seq analysis
  - ChIP-seq analysis
  - Analyses in other Hymenoptera species (Figure S3)
  - Transcription factor analysis (Figure 3)
  - scRNA-seq re-clustering (Figures S4 and S5)
  - Statistics
  - Additional resources

SUPPLEMENTAL INFORMATION

Supplemental information can be found online at https://doi.org/10.1016/j.cell.2021.10.006.

ACKNOWLEDGMENTS

We thank K. Alexander, C. Desplan, M. Goodisman, L. Luense, and A. Petracovici for comments on the manuscript and D. Reinberg for discussions and encouragement. K.M.G. was supported by the NIH (F32GM120933). R.B. acknowledges support from the NIH (DP2MH107055, R21MH123841, and

R01AG071818), the Searle Scholars Program (15-SSP-102), and the 2020 Max Planck-Humboldt Research Award. Funding for this work in S.L.B.'s laboratory was provided by the NIH (R01AG055570).

AUTHOR CONTRIBUTIONS

J.G. designed and performed the majority of the experiments with help from K.M.G. under supervision from R.B. and S.L.B. K.M.G. performed all bioinformatic and statistical analyses. L.S. and E.J.S. contributed unpublished single-cell RNA-seq data and helped with revisions. J.G., K.M.G., and R.B. wrote the manuscript with input from the other authors. All authors edited the manuscript.

DECLARATION OF INTERESTS

The authors declare no competing interests.

Received: November 9, 2020
Revised: July 13, 2021
Accepted: October 7, 2021
Published: November 4, 2021

REFERENCES

Alexa, A., and Rahnenfuhrer, J. (2020). topGO: Enrichment Analysis for Gene Ontology. https://rdrr.io/bioc/topGO/.

Ament, S.A., Corona, M., Pollock, H.S., and Robinson, G.E. (2008). Insulin signaling is involved in the regulation of worker division of labor in honey bee colonies. Proc. Natl. Acad. Sci. USA *105*, 4226–4231.

Anders, S., Reyes, A., and Huber, W. (2012). Detecting differential usage of exons from RNA-seq data. Genome Res. *22*, 2008–2017.

Bates, K.E., Sung, C.S., and Robinow, S. (2010). The unfulfilled gene is required for the development of mushroom body neuropil in Drosophila. Neural Dev. *5*, 4.

Berton, O., McClung, C.A., Dileone, R.J., Krishnan, V., Renthal, W., Russo, S.J., Graham, D., Tsankova, N.M., Bolanos, C.A., Rios, M., et al. (2006). Essential role of BDNF in the mesolimbic dopamine pathway in social defeat stress. Science *311*, 864–868.

Blengini, C.S., Ibrahimian, P., Vaskovicova, M., Drutovic, D., Solc, P., and Schindler, K. (2021). Aurora kinase A is essential for meiosis in mouse oocytes. PLoS Genet. *17*, e1009327.

Bloch, G., Hefetz, A., and Hartfelder, K. (2000). Ecdysteroid titer, ovary status, and dominance in adult worker and queen bumble bees (Bombus terrestris). J. Insect Physiol. *46*, 1033–1040.

Bolger, A.M., Lohse, M., and Usadel, B. (2014). Trimmomatic: a flexible trimmer for Illumina sequence data. Bioinformatics *30*, 2114–2120.

Boulanger, A., Clouet-Redt, C., Farge, M., Flandre, A., Guignard, T., Fernando, C., Juge, F., and Dura, J.M. (2011). ftz-f1 and Hr39 opposing roles on EcR expression during Drosophila mushroom body neuron remodeling. Nat. Neurosci. *14*, 37–44.

Brenman, J.E., Chao, D.S., Gee, S.H., McGee, A.W., Craven, S.E., Santillano, D.R., Wu, Z., Huang, F., Xia, H., Peters, M.F., et al. (1996). Interaction of nitric oxide synthase with the postsynaptic density protein PSD-95 and alpha1-syntrophin mediated by PDZ domains. Cell *84*, 757–767.

Brent, C., Peeters, C., Dietemann, V., Crewe, R., and Vargo, E. (2006). Hormonal correlates of reproductive status in the queenless ponerine ant, Streblognathus peetersi. J. Comp. Physiol. A Neuroethol. Sens. Neural Behav. Physiol. *192*, 315–320.

Brian, M.V. (1974). Caste differentiation in Myrmica rubra: the rôle of hormones. J. Insect Physiol. *20*, 1351–1365.

Butler, A., Hoffman, P., Smibert, P., Papalexi, E., and Satija, R. (2018). Integrating single-cell transcriptomic data across different conditions, technologies, and species. Nat. Biotechnol. *36*, 411–420.

Cáceres, L., Necakov, A.S., Schwartz, C., Kimber, S., Roberts, I.J., and Krause, H.M. (2011). Nitric oxide coordinates metabolism, growth, and development via the nuclear receptor E75. Genes Dev. *25*, 1476–1485.

Chandra, V., Fetter-Pruneda, I., Oxley, P.R., Ritger, A.L., McKenzie, S.K., Libbrecht, R., and Kronauer, D.J.C. (2018). Social regulation of insulin signaling and the evolution of eusociality in ants. Science *361*, 398–402.

Chu, T., Henrion, G., Haegeli, V., and Strickland, S. (2001). Cortex, a Drosophila gene required to complete oocyte meiosis, is a member of the Cdc20/fizzy protein family. Genesis *29*, 141–152.

Conesa, A., Götz, S., García-Gómez, J.M., Terol, J., Talón, M., and Robles, M. (2005). Blast2GO: a universal tool for annotation, visualization and analysis in functional genomics research. Bioinformatics *21*, 3674–3676.

Dobin, A., Davis, C.A., Schlesinger, F., Drenkow, J., Zaleski, C., Jha, S., Batut, P., Chaisson, M., and Gingeras, T.R. (2013). STAR: ultrafast universal RNA-seq aligner. Bioinformatics *29*, 15–21.

Dolezal, A.G., Brent, C.S., Hölldobler, B., and Amdam, G.V. (2012). Worker division of labor and endocrine physiology are associated in the harvester ant, Pogonomyrmex californicus. J. Exp. Biol. *215*, 454–460.

Elekonich, M.M., Schulz, D.J., Bloch, G., and Robinson, G.E. (2001). Juvenile hormone levels in honey bee (Apis mellifera L.) foragers: foraging experience and diurnal variation. J. Insect Physiol. *47*, 1119–1125.

Fang, X., Zhou, J., Liu, W., Duan, X., Gala, U., Sandoval, H., Jaiswal, M., and Tong, C. (2016). Dynamin Regulates Autophagy by Modulating Lysosomal Function. J. Genet. Genomics *43*, 77–86.

Flora, P., Schowalter, S., Wong-Deyrup, S., DeGennaro, M., Nasrallah, M.A., and Rangan, P. (2018). Transient transcriptional silencing alters the cell cycle to promote germline stem cell differentiation in Drosophila. Dev. Biol. *434*, 84–95.

Franklin, T.B., Silva, B.A., Perova, Z., Marrone, L., Masferrer, M.E., Zhan, Y., Kaplan, A., Greetham, L., Verrechia, V., Halman, A., et al. (2017). Prefrontal cortical control of a brainstem social behavior circuit. Nat. Neurosci. *20*, 260–270.

Fussnecker, B., and Grozinger, C. (2008). Dissecting the role of Kr-h1 brain gene expression in foraging behavior in honey bees (Apis mellifera). Insect Mol. Biol. *17*, 515–522.

Ghaninia, M., Haight, K., Berger, S.L., Reinberg, D., Zwiebel, L.J., Ray, A., and Liebig, J. (2017). Chemosensory sensitivity reflects reproductive status in the ant Harpegnathos saltator. Sci. Rep. *7*, 3732.

Glastad, K.M., Graham, R.J., Ju, L., Roessler, J., Brady, C.M., and Berger, S.L. (2020). Epigenetic Regulator CoREST Controls Social Behavior in Ants. Mol. Cell *77*, 338–351.e6.

Gospocic, J., Shields, E.J., Glastad, K.M., Lin, Y., Penick, C.A., Yan, H., Mikheyev, A.S., Linksvayer, T.A., Garcia, B.A., Berger, S.L., et al. (2017). The Neuropeptide Corazonin Controls Social Behavior and Caste Identity in Ants. Cell *170*, 748–759.e12.

Gray, J.D., Kogan, J.F., Marrocco, J., and McEwen, B.S. (2017). Genomic and epigenomic mechanisms of glucocorticoids in the brain. Nat. Rev. Endocrinol. *13*, 661–673.

Grozinger, C.M., and Robinson, G.E. (2007). Endocrine modulation of a pheromone-responsive gene in the honey bee brain. J. Comp. Physiol. A Neuroethol. Sens. Neural Behav. Physiol. *193*, 461–470.

Grozinger, C.M., Sharabash, N.M., Whitfield, C.W., and Robinson, G.E. (2003). Pheromone-mediated gene expression in the honey bee brain. Proc. Natl. Acad. Sci. USA *100* (*Suppl 2*), 14519–14525.

Guo, W., Song, J., Yang, P., Chen, X., Chen, D., Ren, D., Kang, L., and Wang, X. (2020). Juvenile hormone suppresses aggregation behavior through influencing antennal gene expression in locusts. PLoS Genet. *16*, e1008762.

Hammels, C., Pishva, E., De Vry, J., van den Hove, D.L., Prickaerts, J., van Winkel, R., Selten, J.P., Lesch, K.P., Daskalakis, N.P., Steinbusch, H.W., et al. (2015). Defeat stress in rodents: From behavior to molecules. Neurosci. Biobehav. Rev. *59*, 111–140.

Hasanagic, M., van Meel, E., Luan, S., Aurora, R., Kornfeld, S., and Eissenberg, J.C. (2015). The lysosomal enzyme receptor protein (LERP) is not essential, but

is implicated in lysosomal function in Drosophila melanogaster. Biol. Open *4*, 1316–1325.

Hashikawa, K., Hashikawa, Y., Tremblay, R., Zhang, J., Feng, J.E., Sabol, A., Piper, W.T., Lee, H., Rudy, B., and Lin, D. (2017). Esr1^{+} cells in the ventromedial hypothalamus control female aggression. Nat. Neurosci. *20*, 1580–1590.

Huang, Z.-Y., Robinson, G.E., Tobe, S.S., Yagi, K.J., Strambi, C., Strambi, A., and Stay, B. (1991). Hormonal regulation of behavioural development in the honey bee is based on changes in the rate of juvenile hormone biosynthesis. J. Insect Physiol. *37*, 733–741.

Huang, Y., Myers, S.J., and Dingledine, R. (1999). Transcriptional repression by REST: recruitment of Sin3A and histone deacetylase to neuronal genes. Nat. Neurosci. *2*, 867–872.

Ishimoto, H., Sakai, T., and Kitamoto, T. (2009). Ecdysone signaling regulates the formation of long-term courtship memory in adult Drosophila melanogaster. Proc. Natl. Acad. Sci. USA *106*, 6381–6386.

Ishimoto, H., Wang, Z., Rao, Y., Wu, C.F., and Kitamoto, T. (2013). A novel role for ecdysone in Drosophila conditioned behavior: linking GPCR-mediated non-canonical steroid action to cAMP signaling in the adult brain. PLoS Genet. *9*, e1003843.

Jan, L.Y., and Jan, Y.N. (1982). Antibodies to horseradish peroxidase as specific neuronal markers in Drosophila and in grasshopper embryos. Proc. Natl. Acad. Sci. USA *79*, 2700–2704.

Jedlička, P., Ernst, U.R., Votavová, A., Hanus, R., and Valterová, I. (2016). Gene Expression Dynamics in Major Endocrine Regulatory Pathways along the Transition from Solitary to Social Life in a Bumblebee, *Bombus terrestris*. Front. Physiol. *7*, 574.

Jindra, M., Palli, S.R., and Riddiford, L.M. (2013). The juvenile hormone signaling pathway in insect development. Annu. Rev. Entomol. *58*, 181–204.

Jones, P., Binns, D., Chang, H.Y., Fraser, M., Li, W., McAnulla, C., McWilliam, H., Maslen, J., Mitchell, A., Nuka, G., et al. (2014). InterProScan 5: genome-scale protein function classification. Bioinformatics *30*, 1236–1240.

Kapheim, K.M., Jones, B.M., Søvik, E., Stolle, E., Waterhouse, R.M., Bloch, G., and Ben-Shahar, Y. (2020). Brain microRNAs among social and solitary bees. R. Soc. Open Sci. *7*, 200517.

Kim-Ha, J., Smith, J.L., and Macdonald, P.M. (1991). oskar mRNA is localized to the posterior pole of the Drosophila oocyte. Cell *66*, 23–35.

Koyama, T., Texada, M.J., Halberg, K.A., and Rewitz, K. (2020). Metabolism and growth adaptation to environmental conditions in Drosophila. Cell. Mol. Life Sci. *77*, 4523–4551.

Kunwar, P.S., Starz-Gaiano, M., Bainton, R.J., Heberlein, U., and Lehmann, R. (2003). Tre1, a G protein-coupled receptor, directs transepithelial migration of Drosophila germ cells. PLoS Biol. *1*, E80.

Lago, D.C., Humann, F.C., Barchuk, A.R., Abraham, K.J., and Hartfelder, K. (2016). Differential gene expression underlying ovarian phenotype determination in honey bee, Apis mellifera L., caste development. Insect Biochem. Mol. Biol. *79*, 1–12.

Langmead, B., Wilks, C., Antonescu, V., and Charles, R. (2019). Scaling read aligners to hundreds of threads on general-purpose processors. Bioinformatics *35*, 421–432.

Lee, J.H., Budanov, A.V., Park, E.J., Birse, R., Kim, T.E., Perkins, G.A., Ocorr, K., Ellisman, M.H., Bodmer, R., Bier, E., and Karin, M. (2010). Sestrin as a feedback inhibitor of TOR that prevents age-related pathologies. Science *327*, 1223–1228.

Li, H., Handsaker, B., Wysoker, A., Fennell, T., Ruan, J., Homer, N., Marth, G., Abecasis, G., and Durbin, R.; 1000 Genome Project Data Processing Subgroup (2009). The Sequence Alignment/Map format and SAMtools. Bioinformatics *25*, 2078–2079.

Liao, Y., Smyth, G.K., and Shi, W. (2014). featureCounts: an efficient general purpose program for assigning sequence reads to genomic features. Bioinformatics *30*, 923–930.

Lin, H.F., and Wolfner, M.F. (1991). The Drosophila maternal-effect gene fs(1)Ya encodes a cell cycle-dependent nuclear envelope component required for embryonic mitosis. Cell *64*, 49–62.

Lottaz, C., Yang, X., Scheid, S., and Spang, R. (2006). OrderedList–a bioconductor package for detecting similarity in ordered gene lists. Bioinformatics *22*, 2315–2316.

Love, M.I., Huber, W., and Anders, S. (2014). Moderated estimation of fold change and dispersion for RNA-seq data with DESeq2. Genome Biol. *15*, 550.

Lőw, P., Varga, Á., Pircs, K., Nagy, P., Szatmári, Z., Sass, M., and Juhász, G. (2013). Impaired proteasomal degradation enhances autophagy via hypoxia signaling in Drosophila. BMC Cell Biol. *14*, 29.

Lozano, J., and Belles, X. (2011). Conserved repressive function of Krüppel homolog 1 on insect metamorphosis in hemimetabolous and holometabolous species. Sci. Rep. *1*, 163.

Marshall, H., van Zweden, J.S., Van Geystelen, A., Benaets, K., Wäckers, F., Mallon, E.B., and Wenseleers, T. (2020). Parent of origin gene expression in the bumblebee, *Bombus terrestris*, supports Haig's kinship theory for the evolution of genomic imprinting. Evol. Lett. *4*, 479–490.

Mello, T.R.P., Aleixo, A.C., Pinheiro, D.G., Nunes, F.M.F., Cristino, A.S., Bitondi, M.M.G., Barchuk, A.R., and Simões, Z.L.P. (2019). Hormonal control and target genes of ftz-f1 expression in the honeybee Apis mellifera: a positive loop linking juvenile hormone, ftz-f1, and vitellogenin. Insect Mol. Biol. *28*, 145–159.

Minakuchi, C., Zhou, X., and Riddiford, L.M. (2008). Krüppel homolog 1 (Kr-h1) mediates juvenile hormone action during metamorphosis of Drosophila melanogaster. Mech. Dev. *125*, 91–105.

Minakuchi, C., Namiki, T., and Shinoda, T. (2009). Krüppel homolog 1, an early juvenile hormone-response gene downstream of Methoprene-tolerant, mediates its anti-metamorphic action in the red flour beetle Tribolium castaneum. Dev. Biol. *325*, 341–350.

Moreno-Hagelsieb, G., and Latimer, K. (2008). Choosing BLAST options for better detection of orthologs as reciprocal best hits. Bioinformatics *24*, 319–324.

Mouri, A., Ukai, M., Uchida, M., Hasegawa, S., Taniguchi, M., Ito, T., Hida, H., Yoshimi, A., Yamada, K., Kunimoto, S., et al. (2018). Juvenile social defeat stress exposure persistently impairs social behaviors and neurogenesis. Neuropharmacology *133*, 23–37.

Nelson, R.J., Demas, G.E., Huang, P.L., Fishman, M.C., Dawson, V.L., Dawson, T.M., and Snyder, S.H. (1995). Behavioural abnormalities in male mice lacking neuronal nitric oxide synthase. Nature *378*, 383–386.

Niwa, R., Namiki, T., Ito, K., Shimada-Niwa, Y., Kiuchi, M., Kawaoka, S., Kayukawa, T., Banno, Y., Fujimoto, Y., Shigenobu, S., et al. (2010). Non-molting glossy/shroud encodes a short-chain dehydrogenase/reductase that functions in the 'Black Box' of the ecdysteroid biosynthesis pathway. Development *137*, 1991–1999.

Ogawa, S., Tsukahara, S., Choleris, E., and Vasudevan, N. (2020). Estrogenic regulation of social behavior and sexually dimorphic brain formation. Neurosci. Biobehav. Rev. *110*, 46–59.

Ojani, R., Fu, X., Ahmed, T., Liu, P., and Zhu, J. (2018). Krüppel homologue 1 acts as a repressor and an activator in the transcriptional response to juvenile hormone in adult mosquitoes. Insect Mol. Biol. *27*, 268–278.

Opachaloemphan, C., Mancini, G., Konstantinides, N., Parikh, A., Mlejnek, J., Yan, H., Reinberg, D., and Desplan, C. (2021). Early behavioral and molecular events leading to caste switching in the ant *Harpegnathos*. Genes Dev. *35*, 410–424.

Parkhomchuk, D., Borodina, T., Amstislavskiy, V., Banaru, M., Hallen, L., Krobitsch, S., Lehrach, H., and Soldatov, A. (2009). Transcriptome analysis by strand-specific sequencing of complementary DNA. Nucleic Acids Res. *37*, e123.

Patalano, S., Vlasova, A., Wyatt, C., Ewels, P., Camara, F., Ferreira, P.G., Asher, C.L., Jurkowski, T.P., Segonds-Pichon, A., Bachman, M., et al. (2015). Molecular signatures of plastic phenotypes in two eusocial insect species with simple societies. Proc. Natl. Acad. Sci. USA *112*, 13970–13975.

Pecasse, F., Beck, Y., Ruiz, C., and Richards, G. (2000). Krüppel-homolog, a stage-specific modulator of the prepupal ecdysone response, is essential for Drosophila metamorphosis. Dev. Biol. *221*, 53–67.

Peeters, C., and Hölldobler, B. (1995). Reproductive cooperation between queens and their mated workers: the complex life history of an ant with a valuable nest. Proc. Natl. Acad. Sci. USA *92*, 10977–10979.

Peeters, C., Liebig, J., and Holldobler, B. (2000). Sexual reproduction by both queens and workers in the ponerine ant Harpegnathos saltator. Insectes Soc. *47*, 325–332.

Penick, C.A., Liebig, J., and Brent, C.S. (2011). Reproduction, dominance, and caste: endocrine profiles of queens and workers of the ant Harpegnathos saltator. J. Comp. Physiol. A Neuroethol. Sens. Neural Behav. Physiol. *197*, 1063–1071.

Penick, C.A., Brent, C.S., Dolezal, K., and Liebig, J. (2014). Neurohormonal changes associated with ritualized combat and the formation of a reproductive hierarchy in the ant Harpegnathos saltator. J. Exp. Biol. *217*, 1496–1503.

Plyusnina, E.N., Shaposhnikov, M.V., and Moskalev, A.A. (2011). Increase of Drosophila melanogaster lifespan due to D-GADD45 overexpression in the nervous system. Biogerontology *12*, 211–226.

Rabinovich, D., Yaniv, S.P., Alyagor, I., and Schuldiner, O. (2016). Nitric Oxide as a Switching Mechanism between Axon Degeneration and Regrowth during Developmental Remodeling. Cell *164*, 170–182.

Rachinsky, A., Strambi, C., Strambi, A., and Hartfelder, K. (1990). Caste and metamorphosis: hemolymph titers of juvenile hormone and ecdysteroids in last instar honeybee larvae. Gen. Comp. Endocrinol. *79*, 31–38.

Reinking, J., Lam, M.M., Pardee, K., Sampson, H.M., Liu, S., Yang, P., Williams, S., White, W., Lajoie, G., Edwards, A., and Krause, H.M. (2005). The Drosophila nuclear receptor e75 contains heme and is gas responsive. Cell *122*, 195–207.

Rhee, D.Y., Cho, D.Y., Zhai, B., Slattery, M., Ma, L., Mintseris, J., Wong, C.Y., White, K.P., Celniker, S.E., Przytycka, T.M., et al. (2014). Transcription factor networks in Drosophila melanogaster. Cell Rep. *8*, 2031–2043.

Robinson, G.E., Strambi, C., Strambi, A., and Feldlaufer, M.F. (1991). Comparison of juvenile hormone and ecdysteroid haemolymph titres in adult worker and queen honey bees (Apis mellifera). J. Insect Physiol. *37*, 929–935.

Ross-Innes, C.S., Stark, R., Teschendorff, A.E., Holmes, K.A., Ali, H.R., Dunning, M.J., Brown, G.D., Gojis, O., Ellis, I.O., Green, A.R., et al. (2012). Differential oestrogen receptor binding is associated with clinical outcome in breast cancer. Nature *481*, 389–393.

Saha, T.T., Shin, S.W., Dou, W., Roy, S., Zhao, B., Hou, Y., Wang, X.L., Zou, Z., Girke, T., and Raikhel, A.S. (2016). Hairy and Groucho mediate the action of juvenile hormone receptor Methoprene-tolerant in gene repression. Proc. Natl. Acad. Sci. USA *113*, E735–E743.

Sasaki, T., Penick, C.A., Shaffer, Z., Haight, K.L., Pratt, S.C., and Liebig, J. (2016). A Simple Behavioral Model Predicts the Emergence of Complex Animal Hierarchies. Am. Nat. *187*, 765–775.

Schindelin, J., Arganda-Carreras, I., Frise, E., Kaynig, V., Longair, M., Pietzsch, T., Preibisch, S., Rueden, C., Saalfeld, S., Schmid, B., et al. (2012). Fiji: an open-source platform for biological-image analysis. Nat. Methods *9*, 676–682.

Schuh, R., Aicher, W., Gaul, U., Côté, S., Preiss, A., Maier, D., Seifert, E., Nauber, U., Schröder, C., Kemler, R., et al. (1986). A conserved family of nuclear proteins containing structural elements of the finger protein encoded by Krüppel, a Drosophila segmentation gene. Cell *47*, 1025–1032.

Shen, L., and Sinai, M. (2020). GeneOverlap: Test and visualize gene overlaps. https://rdrr.io/bioc/GeneOverlap/.

Sheng, L., Shields, E.J., Gospocic, J., Glastad, K.M., Ratchasanmuang, P., Berger, S.L., Raj, A., Little, S., and Bonasio, R. (2020). Social reprogramming in ants induces longevity-associated glia remodeling. Sci. Adv. *6*, eaba9869.

Shenker, S., Miura, P., Sanfilippo, P., and Lai, E.C. (2015). IsoSCM: improved and alternative 3′ UTR annotation using multiple change-point inference. RNA *21*, 14–27.

Shi, L., Lin, S., Grinberg, Y., Beck, Y., Grozinger, C.M., Robinson, G.E., and Lee, T. (2007). Roles of Drosophila Kruppel-homolog 1 in neuronal morphogenesis. Dev. Neurobiol. *67*, 1614–1626.

Shields, E.J., Sheng, L., Weiner, A.K., Garcia, B.A., and Bonasio, R. (2018). High-Quality Genome Assemblies Reveal Long Non-coding RNAs Expressed in Ant Brains. Cell Rep. *23*, 3078–3090.

Shpigler, H., Patch, H.M., Cohen, M., Fan, Y., Grozinger, C.M., and Bloch, G. (2010). The transcription factor Krüppel homolog 1 is linked to hormone mediated social organization in bees. BMC Evol. Biol. *10*, 120.

Simola, D.F., Graham, R.J., Brady, C.M., Enzmann, B.L., Desplan, C., Ray, A., Zwiebel, L.J., Bonasio, R., Reinberg, D., Liebig, J., and Berger, S.L. (2016). Epigenetic (re)programming of caste-specific behavior in the ant Camponotus floridanus. Science *351*, aac6633.

Singh, A.S., Shah, A., and Brockmann, A. (2018). Honey bee foraging induces upregulation of early growth response protein 1, hormone receptor 38 and candidate downstream genes of the ecdysteroid signalling pathway. Insect Mol. Biol. *27*, 90–98.

Standage, D.S., Berens, A.J., Glastad, K.M., Severin, A.J., Brendel, V.P., and Toth, A.L. (2016). Genome, transcriptome and methylome sequencing of a primitively eusocial wasp reveal a greatly reduced DNA methylation system in a social insect. Mol. Ecol. *25*, 1769–1784.

Stevenson, P.A., and Rillich, J. (2015). Adding up the odds-Nitric oxide signaling underlies the decision to flee and post-conflict depression of aggression. Sci. Adv. *1*, e1500060.

Sunico, C.R., Portillo, F., González-Forero, D., and Moreno-López, B. (2005). Nitric-oxide-directed synaptic remodeling in the adult mammal CNS. J. Neurosci. *25*, 1448–1458.

Supek, F., Bošnjak, M., Škunca, N., and Šmuc, T. (2011). REVIGO summarizes and visualizes long lists of gene ontology terms. PLoS ONE *6*, e21800.

Syed, M.H., Mark, B., and Doe, C.Q. (2017). Steroid hormone induction of temporal gene expression in *Drosophila* brain neuroblasts generates neuronal and glial diversity. eLife *6*, e26287.

Takahashi, A., Chung, J.R., Zhang, S., Zhang, H., Grossman, Y., Aleyasin, H., Flanigan, M.E., Pfau, M.L., Menard, C., Dumitriu, D., et al. (2017). Establishment of a repeated social defeat stress model in female mice. Sci. Rep. *7*, 12838.

Thimgan, M.S., Suzuki, Y., Seugnet, L., Gottschalk, L., and Shaw, P.J. (2010). The perilipin homologue, lipid storage droplet 2, regulates sleep homeostasis and prevents learning impairments following sleep loss. PLoS Biol. *8*, e1000466.

Truman, J.W. (2019). The Evolution of Insect Metamorphosis. Curr. Biol. *29*, R1252–R1268.

Ugajin, A., Kunieda, T., and Kubo, T. (2013). Identification and characterization of an Egr ortholog as a neural immediate early gene in the European honeybee (Apis mellifera L.). FEBS Lett. *587*, 3224–3230.

Uryu, O., Ameku, T., and Niwa, R. (2015). Recent progress in understanding the role of ecdysteroids in adult insects: Germline development and circadian clock in the fruit fly Drosophila melanogaster. Zoological Lett. *1*, 32.

Vanhauwaert, R., Kuenen, S., Masius, R., Bademosi, A., Manetsberger, J., Schoovaerts, N., Bounti, L., Gontcharenko, S., Swerts, J., Vilain, S., et al. (2017). The SAC1 domain in synaptojanin is required for autophagosome maturation at presynaptic terminals. EMBO J. *36*, 1392–1411.

Wang, Y., Azevedo, S.V., Hartfelder, K., and Amdam, G.V. (2013). Insulin-like peptides (AmILP1 and AmILP2) differentially affect female caste development in the honey bee (Apis mellifera L.). J. Exp. Biol. *216*, 4347–4357.

Wang, M., Liu, Y., Wen, T., Liu, W., Gao, Q., Zhao, J., Xiong, Z., Wang, Z., Jiang, W., Yu, Y., et al. (2020). Chromatin accessibility and transcriptome landscapes of Monomorium pharaonis brain. Sci. Data *7*, 217.

Warren, J.T., Petryk, A., Marques, G., Jarcho, M., Parvy, J.P., Dauphin-Villemant, C., O'Connor, M.B., and Gilbert, L.I. (2002). Molecular and biochemical characterization of two P450 enzymes in the ecdysteroidogenic pathway of Drosophila melanogaster. Proc. Natl. Acad. Sci. USA *99*, 11043–11048.

Wei, Q., Lu, X.Y., Liu, L., Schafer, G., Shieh, K.R., Burke, S., Robinson, T.E., Watson, S.J., Seasholtz, A.F., and Akil, H. (2004). Glucocorticoid receptor overexpression in forebrain: a mouse model of increased emotional lability. Proc. Natl. Acad. Sci. USA *101*, 11851–11856.

Wheeler, D.E., and Nijhout, H.F. (1981). Soldier determination in ants: new role for juvenile hormone. Science *213*, 361–363.

Wheeler, D.E., Buck, N., and Evans, J.D. (2006). Expression of insulin pathway genes during the period of caste determination in the honey bee, Apis mellifera. Insect Mol. Biol. *15*, 597–602.

Williams, M.J., Goergen, P., Phad, G., Fredriksson, R., and Schiöth, H.B. (2014). The Drosophila Kctd-family homologue Kctd12-like modulates male aggression and mating behaviour. Eur. J. Neurosci. *40*, 2513–2526.

Yamanaka, N., Rewitz, K.F., and O'Connor, M.B. (2013). Ecdysone control of developmental transitions: lessons from Drosophila research. Annu. Rev. Entomol. *58*, 497–516.

Yamazaki, Y., Shirai, K., Paul, R.K., Fujiyuki, T., Wakamoto, A., Takeuchi, H., and Kubo, T. (2006). Differential expression of HR38 in the mushroom bodies of the honeybee brain depends on the caste and division of labor. FEBS Lett. *580*, 2667–2670.

Yang, C.F., and Shah, N.M. (2014). Representing sex in the brain, one module at a time. Neuron *82*, 261–278.

Yaniv, S.P., and Schuldiner, O. (2016). A fly's view of neuronal remodeling. Wiley Interdiscip. Rev. Dev. Biol. *5*, 618–635.

Young, M.D., and Behjati, S. (2020). SoupX removes ambient RNA contamination from droplet based single cell RNA sequencing data. bioRxiv, 303727.

Zhang, Y., Liu, T., Meyer, C.A., Eeckhoute, J., Johnson, D.S., Bernstein, B.E., Nusbaum, C., Myers, R.M., Brown, M., Li, W., and Liu, X.S. (2008). Model-based analysis of ChIP-Seq (MACS). Genome Biol. *9*, R137.

Zheng, G.X., Terry, J.M., Belgrader, P., Ryvkin, P., Bent, Z.W., Wilson, R., Ziraldo, S.B., Wheeler, T.D., McDermott, G.P., Zhu, J., et al. (2017). Massively parallel digital transcriptional profiling of single cells. Nat. Commun. *8*, 14049.

Please cite this article in press as: Gospocic et al., Kr-h1 maintains distinct caste-specific neurotranscriptomes in response to socially regulated hormones, Cell (2021), https://doi.org/10.1016/j.cell.2021.10.006

STAR★METHODS

KEY RESOURCES TABLE

REAGENT or RESOURCE	SOURCE	IDENTIFIER
Antibodies		
Rabbit anti-horseradish peroxidase (HRP)	Jackson ImmunoResearch	Cat#323-005-021; RRID:AB_2314648
Goat anti-rabbit, Alexa Fluor 488	Thermo Fisher	Cat#A11070; RRID:AB_142134
Alexa Fluor488 AffiniPure Rabbit Anti-Horseradish Peroxidase (HRP)	Jackson ImmunoResearch	Cat# 323-545-021; RRID:AB_2340264
Recombinant Alexa Fluor594 Anti-alpha Tubulin antibody	Abcam	Cat#ab202272
Rabbit anti-Kr-h1 (*Harpegnathos*)	This paper	N/A
Rabbit anti-Met (*Harpegnathos*)	This paper	N/A
Rabbit anti-EcR (*Harpegnathos*)	This paper	N/A
Purified anti-HA.11 epitope tag antibody	Biolegend	Cat#901501; RRID:AB_2565006
Chemicals, peptides, and recombinant proteins		
Neurobasal medium	Thermo Fisher	Cat#21103049
DMEM, high glucose	Thermo Fisher	Cat#11965084
PDS Kit, Papain	Worthington Biochemical	Cat#LK003178
Leupeptin	Sigma-Aldrich	Cat#11017101001
MEM non-essential	Thermo Fisher	Cat#11140050
B-27 Supplement (50X), serum free	Thermo Fisher	Cat#17504044
Insulin-Transferrin-Selenium (ITS -G) (100X)	Thermo Fisher	Cat#41400045
Progesterone	Sigma-Aldrich	Cat#P8783
20-Hydroxyecdysone	Sigma-Aldrich	Cat#H5142
Juvenile hormone III	Sigma-Aldrich	Cat#J2000
Ponasterone A	Abcam	Cat#ab144330
(+)-Methoprene	Abcam	Cat#ab143657
SYBR Gold Nucleic Acid Gel Stain (10,000X Concentrate in DMSO)	Thermo Fisher	Cat#S11494
Critical commercial assays		
Dynabeads Oligo(dT)25	Thermo Fisher	Cat#61005
Dynabeads Protein A	Thermo Fisher	Cat#10002D
Dynabeads Protein G	Thermo Fisher	Cat#10004D
NEBNext Ultra II DNA Library Prep	New England Biolabs	Cat#E7645
in vivo-jetPEI	Polyplus-transfection	Cat#201
Power SYBR Green RNA-to-CT 1-Step Kit	Thermo Fisher	Cat#4389986
QuantiTect Reverse Transcription Kit	QIAGEN	Cat#205313
Power SYBR Green PCR Master Mix	Thermo Fisher	Cat#4367659
Deposited data		
Raw and analyzed data	This paper	GSE161207
Single-cell RNA-seq from *Harpegnathos* brains	Sheng et al., 2020	GSE135513
Bombus terrestris RNA-seq	Marshall et al., 2020	SRP078797
Dinoponera quadriceps RNA-seq	Patalano et al., 2015	SRP044613
Megalopta genalis RNA-seq	Kapheim et al., 2020	SRP079663
Monomorium pharaonis RNA-seq dataset	Wang et al., 2020	SRP239431
Ooceraea biroi RNA-seq dataset	Chandra et al., 2018	SRP148603
Polistes canadensis RNA-seq dataset	Patalano et al., 2015	SRP044613
Polistes dominula RNA-seq dataset	Standage et al., 2016	SRP061693

(*Continued on next page*)

Please cite this article in press as: Gospocic et al., Kr-h1 maintains distinct caste-specific neurotranscriptomes in response to socially regulated hormones, Cell (2021), https://doi.org/10.1016/j.cell.2021.10.006

Continued

REAGENT or RESOURCE	SOURCE	IDENTIFIER
Solenopsis invicta RNA-seq dataset	Chandra et al., 2018	SRP148603
Experimental models: Organisms/strains		
Harpegnathos saltator: wild type	This paper	N/A
Oligonucleotides		
qPCR primer, Kr-h1 F: ACCCTATACCTGCGACATC	This paper	N/A
qPCR primer, Kr-h1 R: ATGTGTAGTTCCATCGTCTTC	This paper	N/A
qPCR primer, Rpl32 F: CGTAGGCGATTTAAGGGTCA	This paper	N/A
qPCR primer, Rpl32 R: TTTCGGAAGCCAGTTGGTAG	This paper	N/A
DsiRNA, nGFP top: rArGrArGrArArArGrGrUrArGrArUr CrCrArArArArArGAA	This paper	N/A
DsiRNA, nGFP bottom: rUrUrCrUrUrUrUrUrGrGrAr UrCrUrArCrCrUrUrUrCrUrCrUrC	This paper	N/A
DsiRNA, Kr-h1 top: rArCrCrUrGrCrUrCrCrArArGrCrAr GrUrUrGrArArGrGrUCC	This paper	N/A
DsiRNA, Kr-h1 bottom: rGrGrArCrCrUrUrCrArArCrUr GrCrUrUrGrGrArGrCrArGrGrUrGrA	This paper	N/A
Software and algorithms		
Blast2GO	Conesa et al., 2005	RRID:SCR_005828
topGO	Alexa and Rahnenfuhrer, 2020	RRID:SCR_014798
REVIGO	Supek et al., 2011	RRID:SCR_005825
bcl2fastq	Illumina	RRID:SCR_015058
STAR	Dobin et al., 2013	RRID:SCR_004463
featureCounts	Liao et al., 2014	RRID:SCR_012919
DESeq2	Love et al., 2014	RRID:SCR_015687
isoSCM v2.0.12	Shenker et al., 2015	N/A
DEXseq	Anders et al., 2012	RRID:SCR_012823
Trimmomatic	Bolger et al., 2014	RRID:SCR_011848
Bowtie2 v2.2.6	Langmead et al., 2019	RRID:SCR_016368
samtools	Li et al., 2009	RRID:SCR_002105
MACS2 version 2.1.1.20160309	Zhang et al., 2008	RRID:SCR_013291
Diffbind	Ross-Innes et al., 2012	RRID:SCR_012918
interproscan	Jones et al., 2014	RRID:SCR_005829
Cell Ranger	Zheng et al., 2017	RRID:SCR_017344
SEURAT	Butler et al., 2018	RRID:SCR_007322
GeneOverlap	Shen and Sinai, 2020	RRID:SCR_018419
OrderedList	Lottaz et al., 2006	RRID:SCR_001834
Fiji	Schindelin et al., 2012	RRID:SCR_002285

RESOURCE AVAILABILITY

Lead contact

Further information and requests for resources and reagents should be directed to and will be fulfilled by the lead contact, Roberto Bonasio (roberto@bonasiolab.org).

Materials availability

Antisera against *Harpegnathos* Kr-h1, Met, and EcR are available from the lead contact upon request.

Data and code availability

- Next generation sequencing data generated for this study have been deposited in the NCBI GEO as SuperSeries GSE161207.
- This paper does not report original code.
- Any additional information required to reanalyze the data reported in this paper is available from the lead contact upon request.

EXPERIMENTAL MODEL AND SUBJECT DETAILS

Harpegnathos husbandry and worker-gamergate transitions

Harpegnathos saltator colonies were housed in polystyrene boxes (Pioneer plastic) with a nest chamber made of plaster kept in a temperature controlled (25°C) ant facility on a 12-h light/dark cycle. Ants were fed every second day with live crickets (*Acheta domesticus* and *Gryllodes sigillatus*). We recapitulated the worker–gamergate transitions as previously described (Gospocic et al., 2017; Sheng et al., 2020). In short, 25 callow females (5 days old) were isolated from their original colonies and transferred with 3 males (7–14 days old) to a new nest without queens or gamergates. Every female ant was individually painted with a unique two-color combination. Ants were carefully observed for 1–2 h every morning and evening for the following two weeks to monitor dueling activities. The intermediate transition time points (Figure 3F) were collected on day 10 and 20 after isolation. After 100 days, all ants were scored for hunting behavior every other day. Four months (120 days) after isolation the whole colony was sacrificed and the gamergate status was determined based on the presence of mature oocytes.

Ant neuronal cell cultures

Primary ant neuronal cultures were generated from central brains of late-stage (P5–P6) *Harpegnathos* pupae. The central brains were collected in neurobasal: DMEM medium (4: 6) with addition of 10 mM HEPES and digested with papain for 5 min at 25°C. Brains were washed once with dissecting media containing 20 μM leupeptin and then twice with dissecting medium without leupeptin. Single-cell suspensions were plated on poly-D-lysine-coated plates in complete growing media (4: 6, neurobasal: DMEM medium with 10 mM HEPES, 1x non-essential amino acids, 1x B27 supplement, 1x insulin-transferrin-selenium, 240 nM progesterone and 5% (v/v) honeybee pupal extract). Cultures were further supplemented with either 2 μM JH3 or 20E. After four days this medium was replaced with one lacking the honeybee pupal extract.

Preparation of honeybee pupal extract for *in vitro* cultures

The honeybee pupal extract was prepared as follows: 13–15 day-old honeybee pupae were removed from the combs and frozen overnight at −80°C. The following day pupae were homogenized in ice-cold neurobasal medium and filtered through 70 μm strainers. To remove debris, the homogenate was centrifuged at 1,500 g for 15 min at 4°C. Honeybee extract was then heat inactivated by incubating at 60°C for 5 min and centrifuged at 1,500 g for 2 h at 4°C. Supernatant was carefully removed from debris and fat, aliquoted, and stored at −80°C.

METHOD DETAILS

Brain dissections

Brains were harvested by dissection in neurobasal medium. The central brain region of interest was isolated by removing the optic lobes, gnathal ganglion, and ~95% of the antennal lobes. The tissue was then processed for RNA- or ChIP-seq.

RNA isolation and sequencing

Harpegnathos brains or ovaries were dissected from single individuals, snap-frozen, and then homogenized in TriPure (Sigma). RNA was purified and its quality visualized on agarose-formaldehyde gels. Typical yields amounted to 0.6 μg total RNA per brain.

For library preparation, polyA+ RNA was isolated from 600 ng total RNA using Dynabeads Oligo$(dT)_{25}$ (Thermo Fisher) and constructed into strand-specific libraries using the dUTP method (Parkhomchuk et al., 2009). UTP-marked cDNA was end-repaired using end-repair mix (Enzymatics), tailed with deoxyadenine using Klenow exo- (Enzymatics), and ligated to adapters with T4 DNA ligase (Enzymatics). Libraries were size-selected with SPRIselect beads (Beckman Coulter) and quantified by qPCR after amplification with custom dual-indexed primers. All sequencing was performed on a NextSeq 500 (Illumina).

Hormone injections

For hormonal stimulation, callow workers (10 days old, referred to as ''immature workers'' in the Results section) were injected with a calibrated glass capillary needle directly into the head, right below the antennae with 100 ng of 20E, 100 ng of JH3, or an equivalent volume of DMSO dissolved in 5% glucose (injected volume ~0.5 μL). 10 h after the injections, central brains were dissected as above in neurobasal medium, and processed for RNA extraction.

For the hunting assay immature workers (as defined above) were acclimated to the social context of the assay by isolating them from their original colony for 24 h before injection. In microcolonies of 9 ants, three were injected with DMSO, three with the hormone analog ponasterone A (PonA), and three with methoprene (meth) in molar amounts equivalent to 100 ng of 20E or 100 ng of JH3, respectively. Behavior was scored after 24 h to allow the injected ants to recover. The DMSO control accounted for potential non-specific effects on behavior and transcriptome due to the process of injection.

Hunting assay

The hunting assay (a.k.a. ''cricket-in-the-tube test'') was performed as previously described (Gospocic et al., 2017) with minor modifications. Ants grouped in micro-colonies (3 PonA + 3 meth + 3 control treated individuals) were acclimatized to the presence of a test

tube for one day before the experiment. On the day of the experiment, the transparent tube was replaced with a new tube without crickets (to score baseline interactions with an empty tube) followed by a tube containing four crickets. Ant behavior was recorded and analyzed offline. We scored as interactions any event wherein an individual spent more than four seconds in the immediate vicinity of the tube either touching its walls or the cotton plug sealing the tube. Attempts to bite the crickets trapped in the tube were also scored as interactions. We counted these events for each individual ant in a 15 min window. Micro-colonies where all individuals of one experimental group (hormone analog- or control-injected) died before recording, or where no interactions were recorded, were excluded from the analysis. The individual ants were tracked by painting different color combinations on their back and the behavioral scores were initially associated exclusively to the color combinations. Only at the end of the experiment the relationships between the color code and experimental treatments were revealed.

Ovary imaging and quantification

For ovary imaging, 6 days after the injection of hormone analogs in the brain, the tissues were dissected in DMEM and fixed in 4% PFA overnight at 4°C. The following day the tissue was blocked and permeabilized for 2 h in blocking buffer (0.5% (v/v) Triton X-100 and 1% (w/v) glycine in phosphate buffered saline (PBS)). The tissue was stained with SYBR Gold (1:5,000) overnight at 4°C with light agitation and washed three times with PBST (0.5% (v/v) Triton X-100 in PBS). Ovaries were imaged in 1x PBS. The ovary activation score was determined based on the developmental stage of the yolky oocytes and nurse cells (see Figure S1G) by an observer who was blinded to the experimental treatments.

Fiji (Schindelin et al., 2012) was used for image processing and quantification of germarium size (Figure S1H). The germarium measurements were performed from SYBR gold-stained ovaries using the Fiji "measure surface area tool" through the widest optical section of the germarium. To obtain arbitrary units, we normalized the size of each germarium to the mean in the control DMSO injections.

Immunofluorescence on neuronal cultures

Primary ant neurons were washed in neurobasal media and fixed in 4% PFA on ice for 20 min. The cells were washed twice with 1x PBS, permeabilized and blocked with blocking buffer (10% (v/v) normal goat serum, 0.1% (v/v) Triton X-100, 1% (w/v) BSA, 0.1% (w/v) glycine in PBS) for 1 h with light agitation. After permeabilization and blocking, cells were incubated with primary antibodies overnight. In some experiments (Figure S2A) we used unconjugated 1:200 anti-HRP antibody (Jackson Immunoresearch, #323-005-021) followed by washes and a 2 h incubation with goat anti-rabbit Alexa488. In other experiments (Figure 2B), cells were stained with directly conjugated anti-HRP Alexa Fluor488 (Jackson Immunoresearch, #323-545-021) and anti-alpha tubulin Alexa Fluor594 (Abcam #ab202272) overnight. After staining, we washed the cells twice with the blocking buffer and counter-stained with DAPI for 30 min, then washed again in PBST (1x PBS + 0.1% (v/v) Triton X-100) and imaged in 1x PBS.

Hormonal stimulation of neuronal cultures

For acute stimulation of neuronal cultures, after 5 days in JH3 or 20E the medium was replaced with one lacking the hormones overnight before adding 2 μM of the opposite hormone (20E in JH3-starved cultures and JH3 in 20E-starved cultures), or DMSO (0.05% final concentration) as a control. To determine the transcriptome of neurons grown in JH3 or 20E at steady-state, we analyzed the respective cultures 30 min after addition of the DMSO control.

Custom antibody production

Antibodies against *Harpegnathos* Kr-h1 (residues 410–580, accession XP_025159603.1), Met (residues 675–923; XP_019696436.1), and EcR (residues 254–441, XP_025154672.1) were raised against recombinant 6xHis-tagged protein fragments. Rabbit immunization was performed by Cocalico Biologicals. MBP-tagged versions of the same antigens were used for affinity purification from the resulting antisera. The antibodies were validated by IP western blot (Figures S5A and S7C).

ChIP-sequencing

For ChIP-seq, three *Harpegnathos* central brains (minus gnathal ganglia and antennal lobes) were resuspended in 300 μL of homogenization buffer (60 mM KCl; 15 mM NaCl; 50 mM HEPES, pH 7.5; 0.1% Triton X-100) with 1% formaldehyde and incubated for 5 min at 25°C with rotation. Formaldehyde was quenched using 250 mM glycine, and brains were gently passed 10–20 times through a 30G insulin syringe. The homogenate was pelleted by centrifugation for 10 min at 1,000 g at 4°C, followed by washing in homogenization buffer, and re-pelleting. The homogenate was then resuspended in 130 μL lysis buffer (50 mM HEPES-KOH, pH 7.5; 140 mM NaCl; 1 mM EDTA; 0.5% Triton X-100; 0.1% Na-deoxycholate; 0.5% N-lauroylsarcosine), and sonicated with a Covaris S220 sonicator in a 130 μL micro tube for 15 min (peak incident power: 105; duty factor: 2%; cycles/burst: 200). The lysate was diluted to 250 μL, equalized according to DNA content (as measured with a Qubit fluorometer), and 25 μL were saved as an input sonication control. A 1:1 mixture of washed and antibody-conjugated protein A and G Dynabeads (2 μg antibody per IP) were added to lysates and incubated overnight at 4°C with rotation in a final volume of 300 μL. The following day, antibody-bead complexes were washed twice in low-salt wash buffer (0.1% Na-deoxycholate; 0.1% SDS; 1% Triton X-100; 10 mM Tris-HCl pH 8.0_{RT}; 1 mM EDTA; 140 mM NaCl), once in high-salt wash buffer (0.1% Na-deoxycholate; 0.1% SDS; 1% Triton X-100; 10 mM Tris-HCl pH 8.0_{RT}; 1 mM EDTA; 360 mM NaCl), twice in LiCl wash buffer (0.5% Na-deoxycholate; 0.5% NP40; 10 mM Tris-HCl pH 8.0_{RT}; 1 mM EDTA; 250 mM LiCl), and

once in TE, followed by two elutions into 75 μL of elution buffer (50 mM Tris-HCl pH 8.0_{RT}; 10 mM EDTA; 1% SDS) at 65°C for 45 min with shaking (1,100 RPM). DNA was purified via phenol:chloroform:isoamyl alcohol (25:24:1) followed by ethanol precipitation. Pelleted DNA was resuspended in 25 μL TE.

Libraries for sequencing were prepared using the NEBNext Ultra II DNA Library Prep Kit for Illumina (NEB E7645), as described by the manufacturer but using half volumes of all reagents and starting material. For PCR amplification of new ChIP-seq targets, the optimal number of cycles was determined using a qPCR side-reaction using 10% of adaptor-ligated, size-selected DNA. These cycle numbers were used for all subsequent replicates of the same ChIP. 13 cycles of PCR were used for Kr-h1, Met, and EcR libraries; 5 cycles were used for input controls.

RNAi for Kr-h1

Kr-h1 knockdowns were performed in immature (10 days old) workers and gamergates for brain RNA-seq (Figure 5) and the hunting assay (Figures 6A and 6B), and in mature (4 months old) workers and gamergates for ovary RNA-seq (Figures 6C–6E).

Custom dicer-substrate short interfering RNAs (DsiRNAs) targeting the Kr-h1 mRNA were synthesized by IDT. DsiRNAs were resuspended at 20 μM and complexed with *in vivo*-jetPEI transfection reagent (Polyplus Transfection) following the manufacturer's instructions. First, equal volumes of 100 μM DsiRNAs and 10% glucose solution were mixed to 10 μl total. Next, 2 μL of *in vivo*-jetPEI reagent was diluted with 8 μL of glucose solution (final concentration of 5%). The two solutions were combined, resulting in 25 μM DsiRNA and incubated for 15 min at 25°C before injections. Immature workers were 10 days old, as defined above. Immature gamergates were obtained by isolating 5-days-old individuals into transition colonies and then selecting active duelers after 5 days of transition, resulting in age-matched, 10-days-old ants committed to the gamergate transition. Each ant was injected with a calibrated glass capillary directly in the head with 0.5 μL of DsiRNA-PEI complexes. To account for the effects of the invasive injection procedure (head puncturing with a glass capillary), we utilized ants injected with DsiRNAs against GFP as controls.

For molecular analyses (RT-qPCR, RNA-seq), ant brains were collected 10 h post-injection. Hunting assays were performed as described above for the hormone analog injections, with the only difference that in this case micro-colonies consisted of only 6 ants, three injected with Kr-h1 DsiRNAs and three controls injected with GFP DsiRNAs.

RT-qPCR for Kr-h1

To assess knockdown of Kr-h1 (Figure 5A) we performed RT-qPCR using the primer sequences indicated in the key resources table and normalizing for the housekeeping gene *Rpl32*. In some experiments we performed RT-qPCR on 20 ng of total RNA in 10 μL reactions using the Power SYBR Green RNA-to-CT 1-Step Kit (Thermo Fisher). In others, we utilized a two-step strategy first generating cDNA from 500 ng RNA with a QuantiTect Reverse Transcription kit (QIAGEN) in a total volume of 40 μL and then using 2 μL per 10 μL qPCR reactions with the Power SYBR Green PCR Master Mix (Thermo Fisher). To compare the extent of knockdown across experiments and castes, data were further normalized to the control brains injected with GFP DsiRNAs.

QUANTIFICATION AND STATISTICAL ANALYSIS

Assignment of gene homology and functional terms

Genes from the NCBI *Harpegnathos saltator* annotation release 102, assembly v8.5 (Shields et al., 2018) were assigned homologs using the reciprocal best BLAST hit method (Moreno-Hagelsieb and Latimer, 2008) to both *D. melanogaster* (r6.16) and *Homo sapiens* (GRCh38) protein-coding genes. The resulting gene symbols are reported as "fly homolog" and "human homolog" in Table S1. For a selected group of genes, we replaced these automatically generated annotations with manual curations by inspecting alignments and phylogeny of the homologous genes in the reference genomes of *D. melanogaster*, *A. mellifera*, *Bombyx mori*, and *Tribolium castaneum*. These manual curations are reported in Table S3.

GO terms were assigned to genes using the blast2go tool (Conesa et al., 2005) using the nr database, as well as InterPro domain predictions. GO enrichment tests were performed with the R package topGO (Alexa and Rahnenfuhrer, 2020), utilizing Fisher's elimination method, and resulting significant terms were entered into REVIGO (Supek et al., 2011) for collapsing of redundant terms.

RNA-seq analysis

Reads were demultiplexed using bcl2fastq2 (Illumina) with the options "–mask-short-adapter-reads 20–minimum-trimmed-read-length 20–no-lane-splitting–barcode-mismatches 0." Reads were aligned to the *Harpegnathos* v8.5 assembly (Shields et al., 2018) using STAR (Dobin et al., 2013). STAR alignments were performed in two passes, with the first using the options "–outFilterType BySJout–outFilterMultimapNmax 20–alignSJoverhangMin 7–alignSJDBoverhangMin 1–outFilterMismatchNmax 999–outFilterMismatchNoverLmax 0.07–alignIntronMin 20–alignIntronMax 100000–alignMatesGapMax 250000," and the second using the options "–outFilterType BySJout–outFilterMultimapNmax 20–alignSJoverhangMin 8–alignSJDBoverhangMin 1–outFilterMismatchNmax 999–outFilterMismatchNoverLmax 0.04–alignIntronMin 20–alignIntronMax 500000–alignMatesGapMax 500000–sjdbFileChrStartEnd [SJ_files]" where "[SJ_files]" corresponds to the splice junctions produced from all first pass runs.

Gene-level read counts were quantified using featureCounts (Liao et al., 2014) with the options "-O -M–fraction -s 2 –p," against a custom NCBI *Harpegnathos* annotation (see following paragraph). Resulting counts were rounded to integers prior to importing into R for DESeq2 analysis in order to account for fractional count values associated with multi-mapping reads.

Please cite this article in press as: Gospocic et al., Kr-h1 maintains distinct caste-specific neurotranscriptomes in response to socially regulated hormones, Cell (2021), https://doi.org/10.1016/j.cell.2021.10.006

Because we observed a large number of genes that possessed truncated 3′UTRs in the *H. saltator* NCBI annotation relative to aligned brain RNA-seq data, we sought to globally amend annotations to account for this. We first aligned all reads as above, but in the second round of alignment included the option "–outSAMattributes NH HI AS nM XS." We then ran isoSCM v2.0.12 (Shenker et al., 2015) assemble with the options "-merge_radius 150 -s reverse_forward" on all alignments. Following this we extracted only 3′ exons from the resulting draft annotations, which were then overlapped with the current NCBI annotation release. We then took the longest predicted 3′ exon/UTR that overlapped with the 3' exon in the current NCBI annotation, and extended this exon according to the isoSCM 3′ exon. Any predicted 3′ exon extension that overlapped an exon of another gene on the same strand was trimmed to 500 bp upstream of the other gene.

Differential gene expression tests were performed with DESeq2 (Love et al., 2014). For all pairwise comparisons the Wald negative binomial test (test = "Wald") was used for determining differentially expressed genes. For hormone injection analyses as well as Kr-h1 knockdown analyses, the injection sample batch was used as a blocking factor. Unless otherwise stated, an adjusted *P*-value cutoff of 0.1 was used to define differentially expressed genes.

For differential exon expression (Figure S7F), DEXSeq (Anders et al., 2012) was run on exon-level counts for all genes using RNA-seq data from mature workers and gamergates, testing for differential exon expression between castes after blocking for gene-level expression differences.

ChIP-seq analysis

Reads were demultiplexed using bcl2fastq2 (Illumina) with the options "–mask-short-adapter-reads 20–minimum-trimmed-read-length 20–no-lane-splitting–barcode-mismatches 0." Reads were trimmed using Trimmomatic (Bolger et al., 2014) with the options "ILLUMINACLIP:[adapter.fa]:2:30:10 LEADING:5 TRAILING:5 SLIDINGWINDOW:4:15 MINLEN:15," and aligned to the *Harpegnathos* v8.5 assembly (Shields et al., 2018) using bowtie2 v2.2.6 (Langmead et al., 2019) with the option "–sensitive-local." Alignments with a mapping quality below 5 and duplicated reads were removed using samtools (Li et al., 2009). Peaks were called using macs2 v2.1.1.20160309 (Zhang et al., 2008) with the options "–call-summits–nomodel -B."

To identify general Kr-h1, Met, and EcR peaks, reads from all replicates, regardless of caste, were used. Only peaks with a fold-enrichment over input > 3 were considered, in order to produce a list of high-confidence peaks to associate to genes. For peak classification, promoters were defined as the region spanning 2 kb upstream and 0.5 kb downstream the transcription start site of a gene. Genes "bound by Kr-h1" were defined as those genes containing a "strong" (fold-enrichment over input > 3) Kr-h1 peak either within the promoter or the gene body.

Differential Kr-h1 ChIP peaks (Figure 4) were called using DiffBind (Ross-Innes et al., 2012) utilizing the option "summits=250" in the dba.count() function, and "bFullLibrarySize=FALSE, bSubControl=TRUE, bTagwise=FALSE" for dba.analyze(). All peaks called by macs2 were used regardless of fold enrichment. For DiffBind testing the DESeq2 algorithm (Wald negative binomial test) with blocking was used, and ChIP replicate was used as the blocking factor while testing for caste differences. A *P*-value of 0.01 was used as threshold to define differential binding.

To generate genome browser tracks and heatmaps, RPM (reads per million) were calculated for each biological replicate and then averaged.

Analyses in other Hymenoptera species (Figure S3)

For comparisons with other species' RNA-seq data, we used the following RNA-seq SRA datasets and comparisons: *B. terrestris* (SRP078797), dominant reproductive versus foragers (Marshall et al., 2020); *D. quadriceps* (SRP044613), alpha versus low (Patalano et al., 2015); *M. genalis* (SRP079663), queen versus worker (Kapheim et al., 2020); *M. pharaonis* (SRP239431), queen versus worker (Wang et al., 2020); *O. biroi* (SRP148603), reproductive versus non-reproductive workers (Chandra et al., 2018); *P. canadensis* (SRP044613), gyne versus worker (Patalano et al., 2015); *P. dominula* (SRP061693), gyne versus worker (Standage et al., 2016); *S. invicta* (SRP148603), queen versus forager (Chandra et al., 2018). Reads were mapped to the current Refseq release of the relevant genome and annotation, and gene-level counts quantified as described for *Harpegnathos*. DESeq2 was used to compare reproductive versus non-reproductive castes. Genes from each species were associated with *Harpegnathos* using reciprocal best hits by BLAST. Only genes with unambiguous 1:1 reciprocal homologs between each species and *Harpegnathos* were considered in the comparisons (hence the difference in numbers for the *Harpegnathos* neuronal cultures gene set in Figure S3).

Transcription factor analysis (Figure 3)

For identification of hormone-induced transcription factors, the amino acid sequences of all protein-coding genes were first scanned with InterProScan (Jones et al., 2014) and all genes with a significant domain hit to a known DNA binding domain (Zf_C2H2, homeobox_like, HTH, WH, LIM_type, HMG_box, Zf_GATA, Pax, bHLH, BTB_POZ, POU, bZIP, p53_like,Zf_TFIIB_type, MADS_box, Znf_hrmn_rcpt) were annotated as putative DNA-binding factors. The resulting annotations are reported in Table S4.

All these genes were assessed for differential expression (adjusted $p < 0.1$) in any of the three hormone switch time points (0.5, 6, and 24 h) compared to the baseline (30 min DMSO). For transcription factor heatmaps (Figures 3B, 3C, S2F, and S2G), normalized counts (DESeq2) were *z*-score transformed and clustered using the complete linkage clustering method.

scRNA-seq re-clustering (Figures S4 and S5)

For scRNA-seq analyses we used 10x Genomics reads from Sheng et al. (2020). We utilized cellranger (Zheng et al., 2017) with the revised *Harpegnathos* annotation inclusive of the extended 3′ UTRs described above, due to the fact that 10x scRNA-seq data is highly biased toward the 3′. We then used Seurat (Butler et al., 2018) to perform clustering and differential testing.

For clustering we only included cells with nFeature_RNA > 500 and < 5,000, and with < 5% mitochondrial reads. We next used the SCTransform method within Seurat to combine samples, using 3,000 integration features excluding certain genes (see below). We then selected 2,500 variable features for PCA, but excluded a list of 1,414 genes related to mitochondrial function, tRNA synthesis, cellular respiration, glycolysis and ribosomal functions, as well as a list of manually curated steroid receptors, and genes responsive to JH3 or 20E in the neuronal cultures (Table S5). This was done to obtain consistent clustering across samples, guided by cell type rather than metabolic or hormonal status.

PCA and UMAP clustering were performed using the top 30 principal components, and clusters were determined using a resolution of 1.0 and the Louvain algorithm. For determination of per-cluster caste differential genes, the FindMarkers function of Seurat was run on each cluster, comparing cells from workers and gamergates using the MAST test and controlling for the latent variables nFeature_RNA (number of features with data) and mitochondrial reads. For Figure S2E, the function quickMarkers from the soupX package (Young and Behjati, 2020) was used to determine cluster markers, then the top 200 markers for each cluster were analyzed.

For UMAP significance plots, the *P*-values from Fisher's exact tests on the overlaps between bulk *in vitro* differentially expressed genes (Figure S4C) or genes differentially bounds by Kr-h1 *in vivo* (Figure S5D) and genes differentially expressed at the cluster level in the scRNA-seq were log-transformed and plotted in a cluster-specific way on the UMAPs.

Statistics

Sample size and statistical tests are indicated in the figure legends. Unless otherwise noted all statistical tests were two-sided. All replicates were obtained by measuring distinct samples (biological and/or experimental replicates) and not by measuring multiple times the same sample (technical replicates). Boxplots were drawn using default parameters in R (center line, median; box limits, upper and lower quartiles; whiskers, 1.5x interquartile range). For testing significance of gene overlaps, we used the GeneOverlap R package (Shen and Sinai, 2020) and the R package OrderedList (Lottaz et al., 2006). For the latter, gene lists were ranked according to |log-fold-change| x $\log_{10}$(*P*-value) (Gospocic et al., 2017). When testing lists of differentially expressed genes for their overlap, those genes for which DESeq2 returned an "NA" as the adjusted *P*-value in any of the samples being compared were excluded.

For analysis of behavioral data at the individual ant level, which is discrete in nature (number of cricket interactions displayed by each ant in the given time window), we first assessed the fit of different distributions to our empirical data. The behavioral scores were over-dispersed compared to a simple Poisson function and best modeled by a negative binomial distribution. Individual ant cricket test scores were modeled as a function of treatment, blocking for experimental batch and individual colony box.

Additional resources

No additional resources were generated for this study.

Supplemental figures

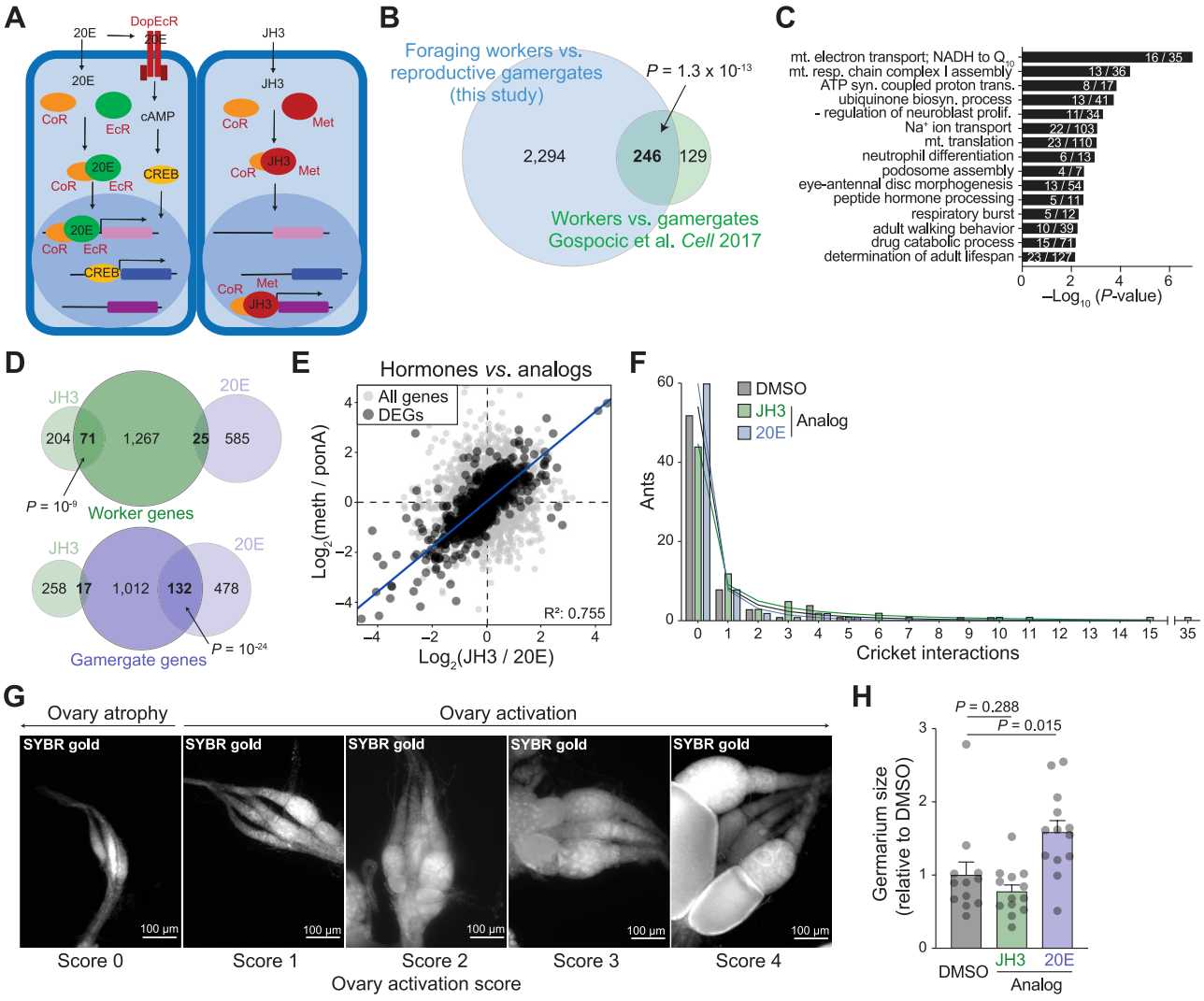

Figure S1. JH3 and 20E effects on brain gene expression and caste traits, related to Figure 1

(A) Scheme of 20E (left) and JH3 (right) signaling. The hormones diffuse through the cell membrane and bind to their cytosolic receptors, EcR or Met. Ligand binding induces the association of the receptors with co-receptors (CoR) and their translocation into the nucleus, where they regulate gene expression. 20E can also signal through a G protein-coupled receptor, DopEcR, which activates CREB via cyclic AMP (cAMP).

(B) Overlap of differentially expressed genes in the central brain minus gnathal ganglia and antennal lobes of the mature castes, as identified in this study (actively foraging workers versus dominant reproductive gamergates, see Figure 1A), and caste-biased genes previously identified in the non-visual brains (central brain including gnathal ganglia and antennal lobes) of generic workers versus gamergates (Gospocic et al., 2017). *P*-value is from a Fisher's exact test.

(C) Top 15 "biological process" GO terms enriched among differentially expressed genes in the brains of mature workers versus gamergates. Numbers within bars correspond to the number of genes with each GO term found in the gene set and in all testable (detected) genes.

(D) Overlap of genes upregulated in worker brains (top) or gamergate brains (bottom) with genes stimulated by injections of JH3 versus 20E *in vivo* (from Figure 1C). *P*-values are from Fisher's exact tests.

(E) Scatterplot showing the correlation between log-fold-change in gene expression upon injections of the natural hormones (JH3 or 20E, x axis) and, on the y axis, the analogs used for the functional assays in Figure 1: methoprene (meth) or ponasterin A (ponA). Differentially expressed genes (DEGs; adj. $p < 0.1$) in either comparison are shown in semi-transparent black.

(F) Histogram plot showing the number of individual ants (y axis) exhibiting a given number of interactions in the observation window (x axis) from Figure 1H. The treatment groups are shown in separate bars and color-coded. The negative binomial fit for each group is shown by the solid lines in matching colors.

(G) Microphotographs of ovaries isolated from individuals six days after hormone or control injections counterstained with SYBR gold. The ovary scores for Figure 1I were determined according to the presence of different stages of oocytes, nurse cells, and overall ovary size. Representative examples for each score are shown.

(H) The surface area of the germarium was measured and normalized to the average observed in the DMSO-injected controls. Bars represent mean + SEM. *P*-values are from ANOVA and Holm-Sidak test.

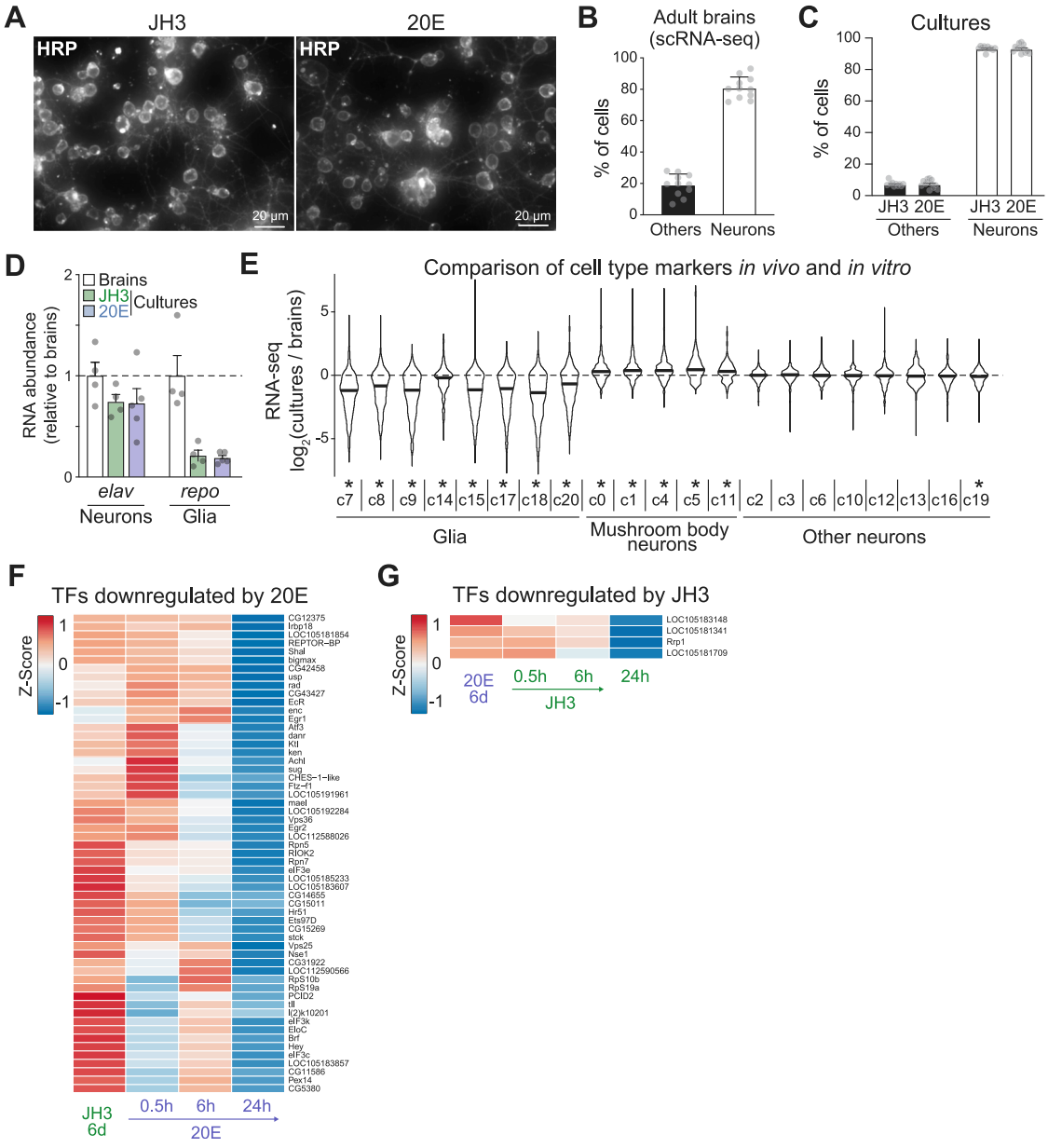

Figure S2. Composition and transcriptional response of primary ant neuronal cultures, related to Figures 2 and 3

(A) Immunofluorescence on primary cell cultures from pupal brains grown in the indicated conditions and stained for the pan-neuronal marker HRP.

(B) Relative abundance of neurons and glia in adult *Harpegnathos* brains as determined by single cell RNA-seq (Sheng et al., 2020). Bars represent mean + SEM.

(C) Percentage of cells positive (neurons) or negative (others) for HRP staining in JH3 or 20E conditions. Bars represent the mean + SEM.

(D) Expression of *elav* and *repo* in pupal brains at harvesting compared to neuronal cultures in JH3 and 20E conditions, as measured by RNA-seq. Levels for each gene are expressed relative to the average in pupal brain (set to 1, dashed line). Bars represent mean + SEM.

(E) Expression of markers for different neuronal and glia subtype (as determined from reanalysis of single-cell RNA-seq) (Sheng et al., 2020) in pupal brains at harvesting (*in vivo*) and after 6 days of *in vitro* culture. Violin plots show the distribution of the ratios for *in vitro* versus *in vivo* expression levels for the top 200 marker genes for each cluster. *p < 0.05 from Wilcoxon signed-rank tests.

(F and G) RNA-seq expression heatmaps of transcription factors downregulated in response to the hormonal switches *in vitro* (adj. p < 0.1 in at least one of the time points compared to baseline). Heatmaps show *Z*-scores of DESeq2-normalized counts. Rows were ordered by hierarchical clustering. Data from ≥ 4 biological replicates per condition.

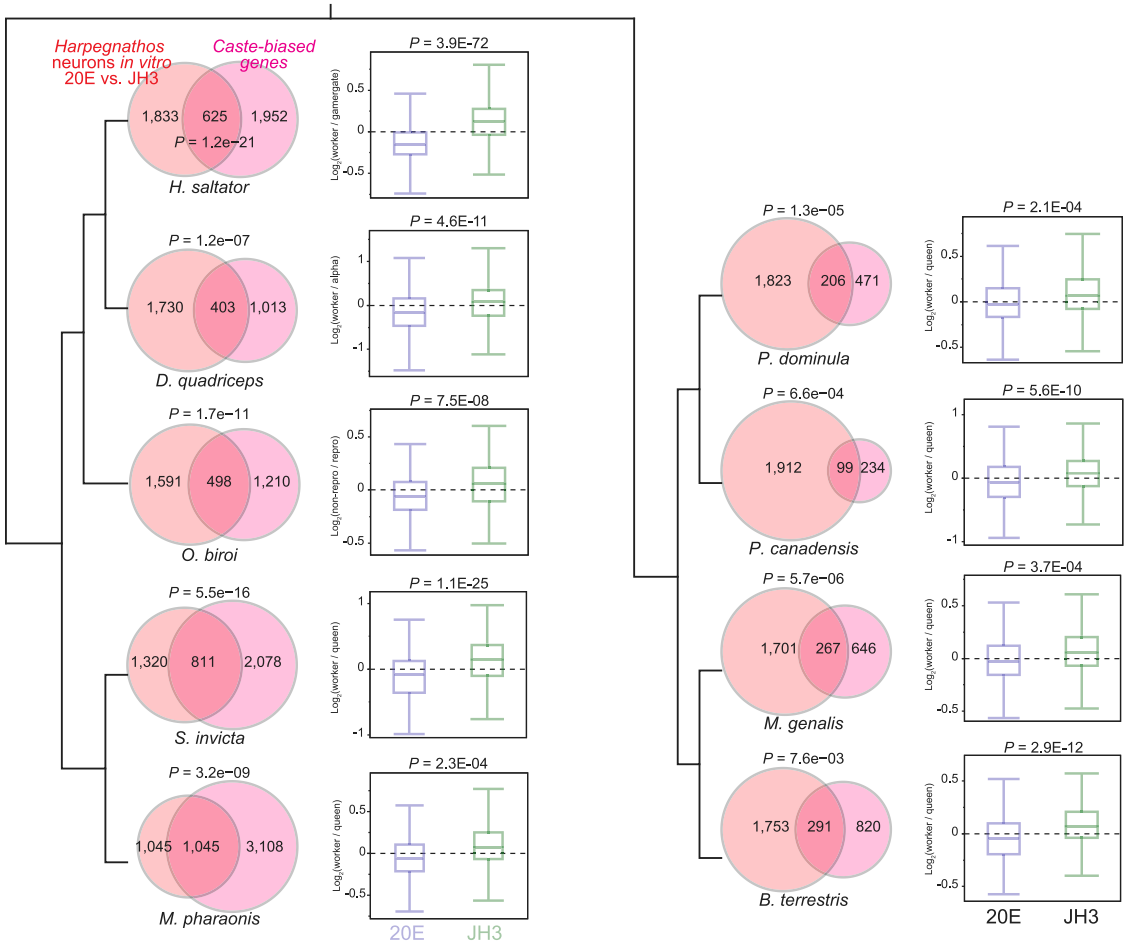

Figure S3. Conservation of JH3 and 20E signatures in Hymenoptera castes, related to Figure 2

Overlaps between caste-biased genes in different Hymenoptera species with the genes differentially induced by JH3 and 20E in *Harpegnathos* neurons *in vitro*. Also shown are boxplots of RNA-seq $\log_2$(fold-change) of expression in non-reproductive versus reproductive castes in the different species comparing genes induced by JH3 or 20E in *Harpegnathos* neurons. *P*-values above Venn diagrams are from Fisher's exact tests, and *P*-values above boxplots are from Wilcoxon signed rank tests. Only genes with unambiguous 1:1 reciprocal homologs between each species and *Harpegnathos* were considered in the comparisons (hence the difference in numbers for the *Harpegnathos* neuronal cultures gene set).

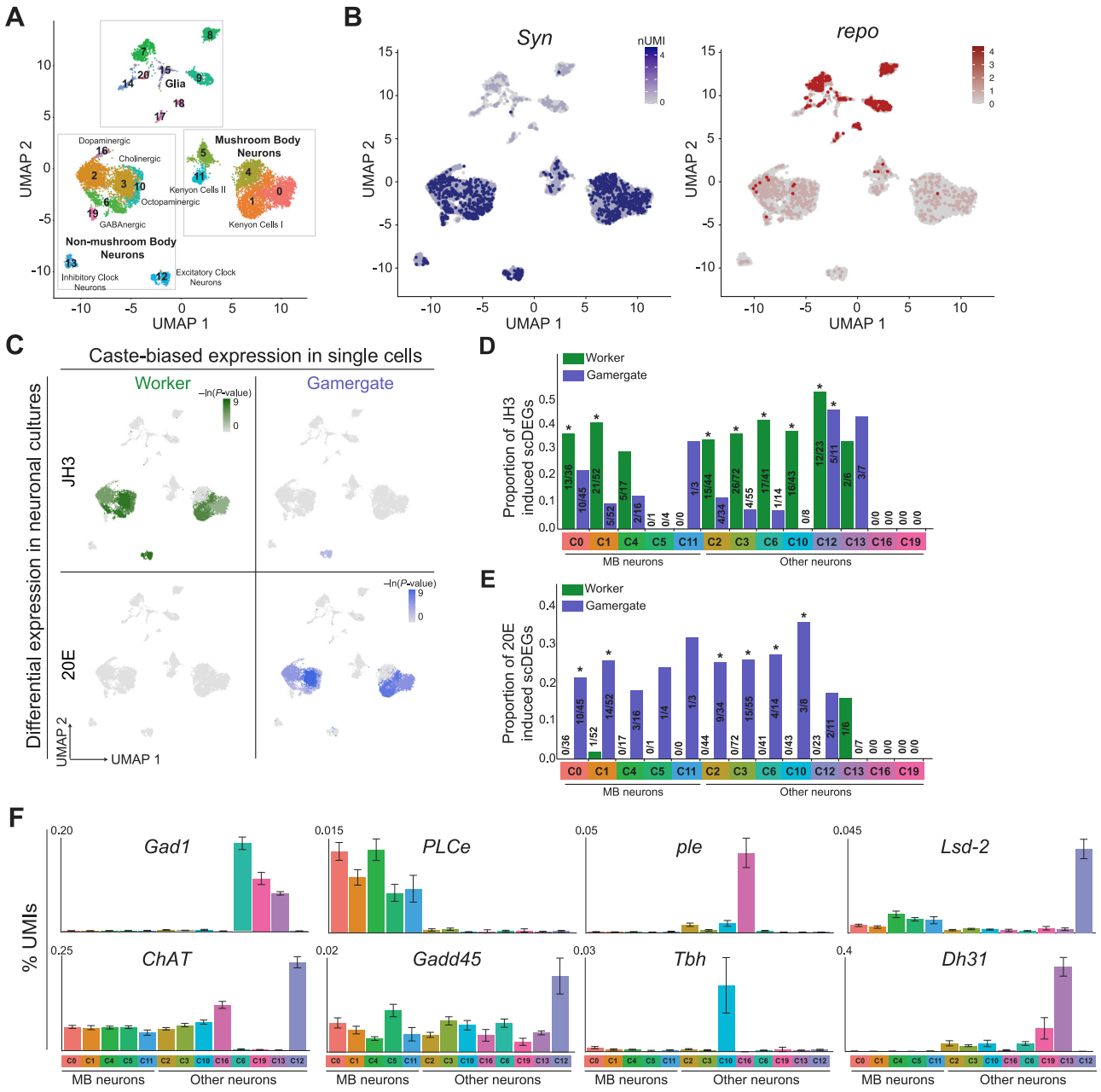

Figure S4. *In vivo* single-cell analyses for JH3- and 20E-induced genes *in vitro*, related to Figure 2

(A) Annotated UMAP visualization of single-cell RNA-seq dataset from *Harpegnathos* brain (Sheng et al., 2020) obtained by pooling all cells from 6 worker and 5 gamergate replicates and re-clustering with an updated annotation.

(B) Heatmap plotted over global UMAP showing normalized UMIs per cell for a neuronal marker (*Syn*) in blue and a glial marker (*repo*) in red.

(C) Heatmap plotted over global UMAP showing the overlap of genes differentially expressed *in vitro* in JH3 or 20E conditions at steady state with caste-specific genes at the single-cell level. The clusters are shaded based on the *P*-values of the Fisher's exact tests for the overlaps.

(D and E) Bar graphs showing proportions of genes differentially expressed at the single-cell level (scDEGs) between workers and gamergates that overlap JH3- (D) or 20E- (E) induced genes in the cell cultures. *, *P*-value < 0.05 from Fisher's exact tests.

(F) Expression across neuronal clusters of selected marker genes used for the annotation.

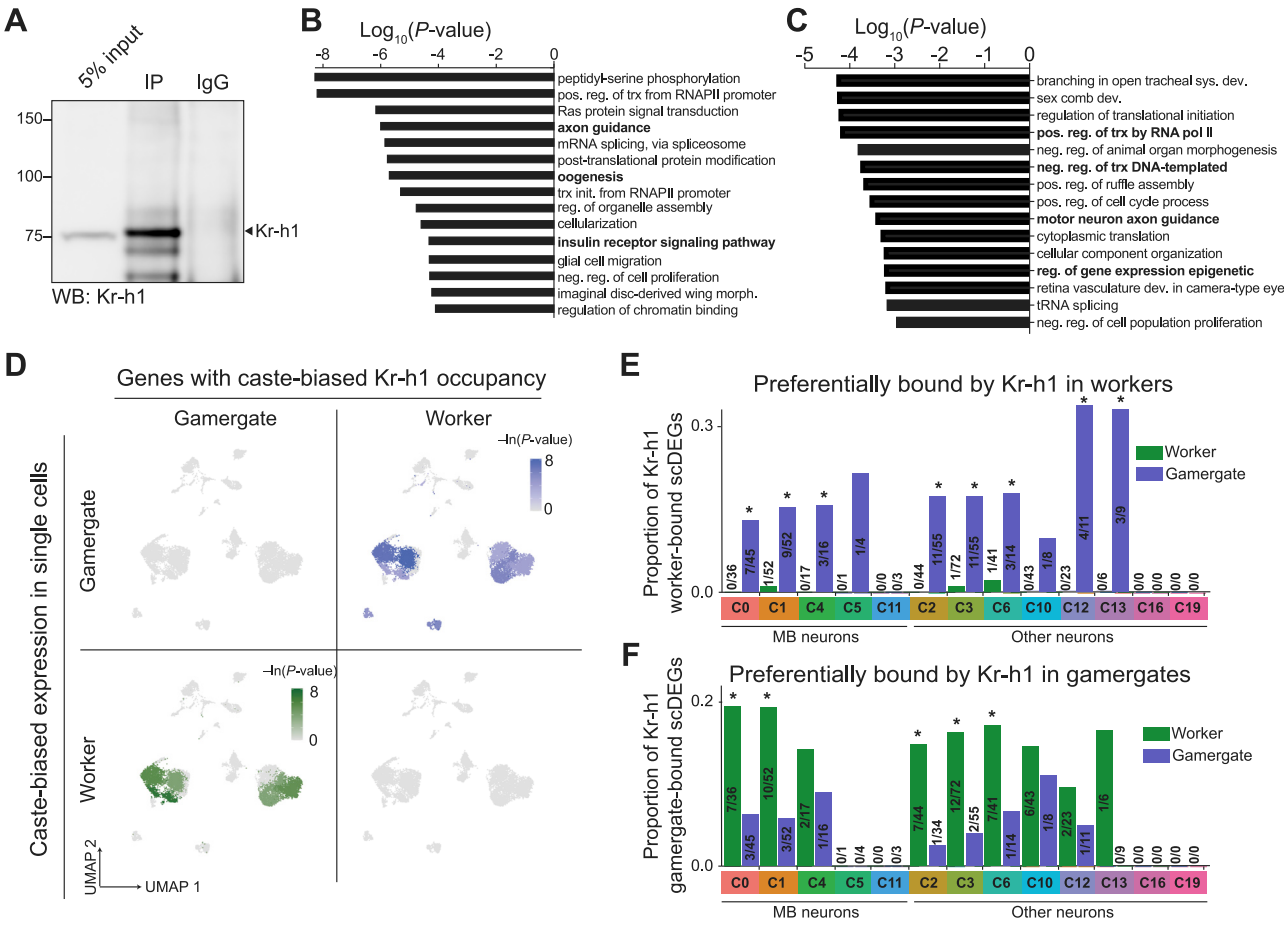

Figure S5. Analyses on genes bound by Kr-h1, related to Figure 4

(A) Proteins were extracted from *Harpegnathos* brains, subjected to immunoprecipitation with the Kr-h1 antibody and then separated on SDS-PAGE. The arrowhead indicates the Kr-h1 band (predicted MW: 71 kDa).

(B) Top 15 "biological process" GO terms significantly enriched for genes containing a Kr-h1 peak. Terms mentioned in the text are in bold.

(C) Top 15 "biological process" GO terms associated with genes differentially bound by Kr-h1 in worker and gamergate brains (from Figure 4D). Terms related to transcriptional and epigenetic regulation as well as neuronal remodeling are in bold.

(D) Heatmap plotted over global UMAP showing enrichment of genes with preferential Kr-h1 binding in gamergate or worker brains among genes expressed in a caste-biased manner at the single-cell level. The clusters are shaded based on the log-transformed *P*-values for the overlaps from Fisher's exact tests.

(E and F) Bar graphs showing proportions of genes differentially bound by Kr-h1 in workers versus gamergates that overlap with genes differentially expressed in worker and gamergates at the single-cell level (scDEGs). *, *P*-value < 0.05, Fisher's exact test.

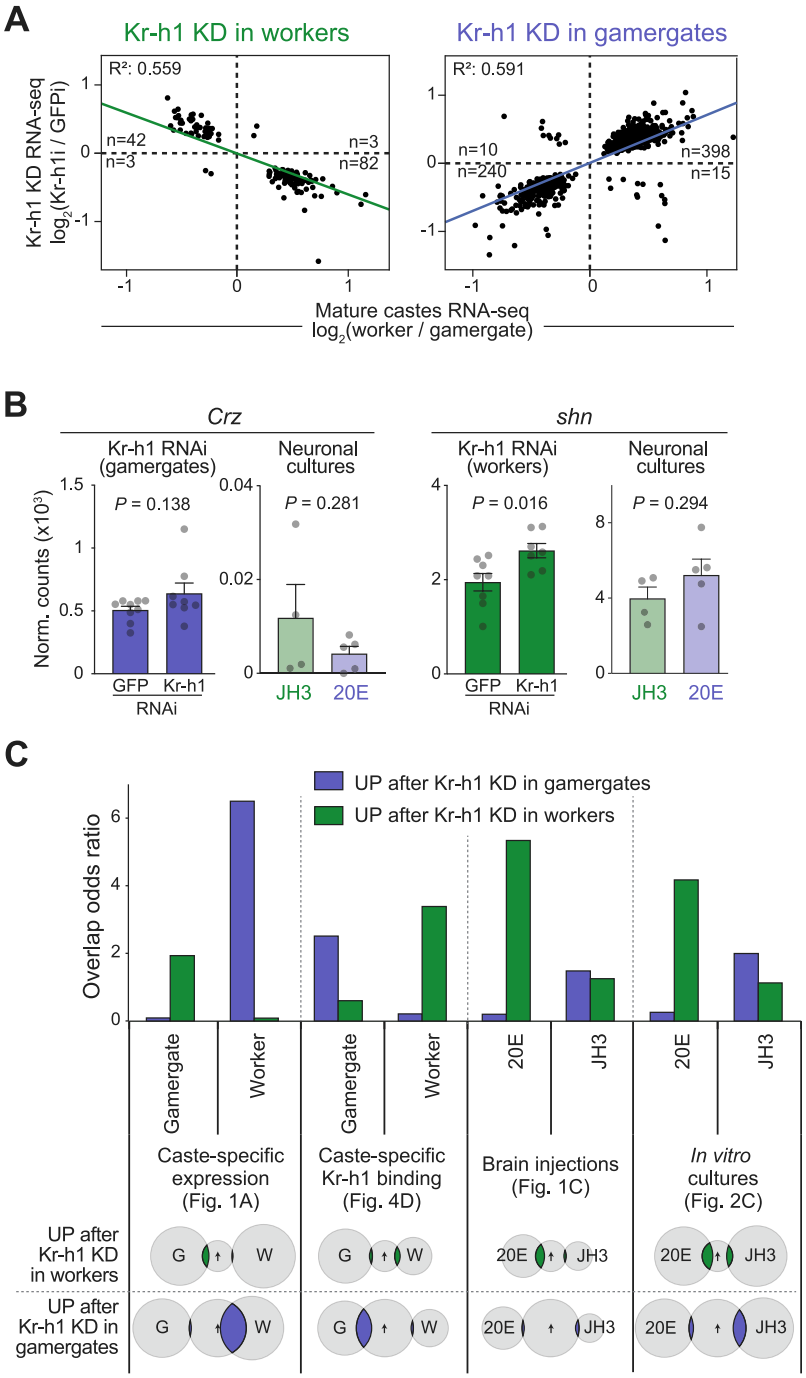

Figure S6. Gene expression levels and overlaps of Kr-h1 target genes, related to Figure 5

(A) Scatterplots showing the correlation between changes in gene expression upon Kr-h1 knockdown in immature workers (left) or immature gamergates (right) with differential expression of genes in the brains of mature workers versus gamergates (x axis).

(B) Expression levels (DESeq2-normalized counts) for two additional Kr-h1 target genes in the brain after knockdown of Kr-h1 or GFP control in immature gamergates (left) or workers (right). Bars represent mean + SEM *P*-values are from Student's t tests.

(C) Odds ratios from Fisher's exact tests on the overlaps between genes upregulated in the brain after Kr-h1 knockdown in immature workers (green) or immature gamergates (blue) versus (left to right) genes differentially expressed in mature castes; genes with differential binding of Kr-h1 by ChIP-seq in mature castes; genes differentially affected by JH3 and 20E injections in the brain; genes differentially expressed in neurons cultured in presence of JH3 or 20E *in vitro*. Below the bar plots, the corresponding Venn diagrams for the overlaps are shown.

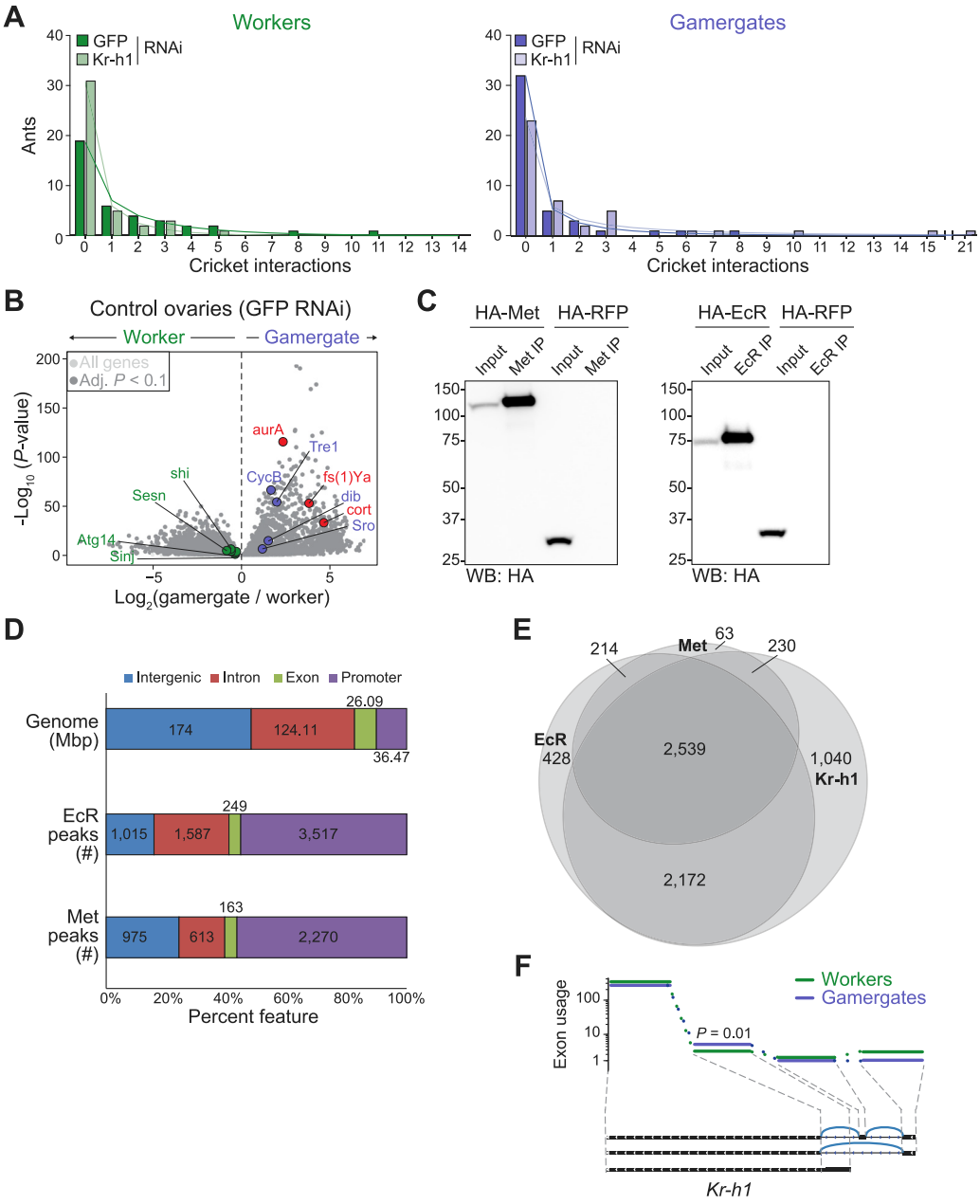

Figure S7. Caste-specific targeting and function of Kr-h1, related to Figures 6 and 7

(A) Histogram plot showing the number of individual ants (y axis) exhibiting a given number of interactions in the observation window (x axis), from Figure 6B. The treatment groups are shown in separate bars and color-coded. The negative binomial fit for each group is shown by the solid lines.

(B) RNA-seq from ovaries of mature (4 months old) control GFPi-injected workers and gamergates. Genes discussed in the text are highlighted in colors. Data from 5 (workers) and 6 (gamergates) biological replicates.

(C) Quality control for anti-Met and anti-EcR antibodies. HA-fused Met and EcR were expressed in HEK293 cells and immunoprecipitations were performed with the respective antibodies followed by SDS-PAGE and western blot against HA. An irrelevant control protein also fused to HA (HA-RFP) is shown as negative control.

(D) Proportion of EcR and Met peaks (fold over input > 3) within major genomic features.

(E) Overlap of Met, EcR, and Kr-h1 gene targets.

(F) Alternative exon usage analysis for Kr-h1. Top: read coverage for exons 1–4 in the brains of mature workers versus gamergates. Bottom: sashimi plot showing the possible Kr-h1 transcriptional isoforms. Adjusted *P*-value is from DEXseq.